

CHAPTER III

THEORETICAL INVESTIGATIONS ON  
THE OPTICAL ABSORPTION, MAGNETIC SUSCEPTIBILITY,  
g-VALUES AND MAGNETIC HEAT CAPACITY  
OF SOME RARE-EARTH COMPLEXES

This chapter deals with the interpretation of the optical, thermal and magnetic behaviours of some rare-earth complexes. A number of theoretical calculations on optical absorption<sup>89</sup> and e.p.r.<sup>90,91</sup> spectra of various rare-earth complexes have been done earlier. Theoretical works on the susceptibility of some RE complexes have also been done earlier<sup>92-95</sup>. Special mention may be made to the RE chlorides and ethyl sulphates which have been studied extensively and parameters giving a good fit to the optical results have been already evaluated. Some workers<sup>3,92-95</sup> also tried to fit the magnetic data. But still we find that there is no unified approach to explain the magnetic susceptibilities, g-values and the CF levels of RE crystals with a single set of parameters. Sometimes, this may be due to insufficient data. But in many cases we find that no rigorous approach to interpret simultaneously the e.p.r., the magnetic susceptibility and the optical absorption data of RE complexes have been taken recourse to. While rigorous approach by using intermediate coupling and J-mixing is found in the case of interpreting many optical results, the theoretical interpretation of magnetic susceptibility and e.p.r. results of same RE ions considered only the lowest Russel-Saunders term. We have chosen the  $4f^2$ ,  $4f^3$  and  $4f^{12}$  electronic configurations for our theoretical study on the optical absorption, the magnetic

susceptibility results, the g-values and in one case the magnetic heat capacity of a specific complex. In the present chapter we confine our attention mainly to some RE ethyl sulphates and double nitrates of the above mentioned system such as (i)  $\text{Nd}^{3+}$  ethyl sulphate, (ii)  $\text{Tm}^{3+}$  ethyl sulphate, (iii)  $\text{Pr}^{3+}$  ethyl sulphate, (iv)  $\text{Pr}^{3+}$  double nitrate. These complexes received attention fairly long ago, but a unified theory to interpret consistently and simultaneously all the different experimental results is still lacking. We enumerate the reasons for the choice of these complexes :

(1) The magnetic susceptibility and anisotropy data are available in full details but the correct interpretation was not found

(2) Due to the simple electronic configuration it is easy to diagonalise the hamiltonian giving rigorous solution of the eigenvalue problem. The intermediate coupling and different J-mixing under the crystal field are then automatically taken into account in the rigorous solution.

(3) The interpretation of the optical data of RE ethyl sulphates or double nitrates has been reliably done earlier. But in most cases the attempts were not done to test whether the interpretation of the optical result is also consistent with the magnetic susceptibility results and the g-values. i.e., whether the parameters which reproduce the CF levels faithfully can also successfully explain the magnetic susceptibilities and the g-values or not .

(4) Some of the early CF calculations regarding the RE ethyl sulphates or double nitrates are in R.S. coupling scheme which are totally inadequate to explain the other experimental data like magnetic susceptibility and the g-values.

So this invokes us to take up these problems. Our aim is to see how CF theory can successfully explain the optical absorption spectra and then to see whether the same theory can reproduce the magnetic and e.p.r data faithfully. During calculation we have considered not only the intermediate coupling scheme but also the J-mixing and in case of  $4f^2$  and  $4f^{12}$  a rigorous approach which considers diagonalisation of the complete energy matrix has been adopted. The results were then used to calculate the susceptibility and the g-values (for  $4f^{12}$  system magnetic heat capacity is also calculated). In all cases we made an attempt to explain the optical absorption results, the susceptibility and g-values simultaneously from a single set of parameters.

### III.1. INTERPRETATION OF THE MAGNETIC BEHAVIOURS OF NEODYMIUM ETHYL SULPHATE

#### III.1.1. INTRODUCTION

In this section we shall make an attempt to give a theoretical interpretation of the magnetic susceptibility

values at different temperature, g values and also the optical spectra of Neodymium ethyl sulphate and we shall show that all these experimental results can be successfully explained by using a unique set of theoretical parameters, which will be evaluated from the experimental results themselves. Elliott and Stevens<sup>3</sup> were the first to give a theoretical interpretation of the e.p.r results of rare-earth ethylsulphates in terms of the crystal field theory. They considered a crystal field of  $D_{3h}$  symmetry of the rare-earth ions in the ethyl sulphate lattice and in the case of NES (neodymium ethylsulphate) they achieved some success in interpreting the e.p.r and magnetic susceptibility data with the following set of crystal field parameters:  $B_2^0 = -15 \text{ cm}^{-1}$ ,  $B_4^0 = -35 \text{ cm}^{-1}$ ,  $B_6^0 = -60 \text{ cm}^{-1}$  and  $B_6^6 = 640 \text{ cm}^{-1}$ . The theory used the Russel Saunder's (R.S.) coupling scheme and mixing of only  $^4I_{11/2}$  with the free-ion ground level  $^4I_{9/2}$ . The predicted crystal field energy levels were found later to deviate considerably from the observed optical data of Gruber and Satten<sup>96</sup> for the concentrated crystals of NES not only in magnitude but also in the order of some of the levels. It now appears that Elliott and Stevens<sup>3</sup> tried to fit the e.p.r results of diluted crystal on the one hand and magnetic data of concentrated crystal on the other with the same set of parameters. The calculated g-values (i.e.  $g_{||} = 3.56$ ,  $g_{\perp} = 2.12$ ), are not in good agreement with the latest experimental result

$g_{\parallel} = 3.594$  and  $g_{\perp} = 2.039$  of Fisher et al<sup>97</sup> for the concentrated crystals of NES and the fitting of magnetic data is also not very satisfactory.

Gruber and Satten<sup>96</sup>, in their theory, took intermediate coupling (IC) scheme into account although in an indirect way and used the mixing of the J-levels  ${}^4I_{11/2}$ ,  ${}^4I_{13/2}$  and  ${}^4I_{15/2}$  with  ${}^4I_{9/2}$ . With the set of parameters  $B_2^0 = 58.4 \text{ cm}^{-1}$ ,  $B_4^0 = -68.2 \text{ cm}^{-1}$ ,  $B_6^0 = -42.7 \text{ cm}^{-1}$  and  $B_6^6 = 595 \text{ cm}^{-1}$ , a set quite different from that of Elliott and Stevens<sup>3</sup>, they were able to fit the observed crystal field levels in their optical absorption experiment on concentrated crystals of NES within a mean deviation of only  $4 \text{ cm}^{-1}$ . However, they did not test whether the parameters quoted by them could faithfully reproduce the observed g-values and magnetic susceptibilities. Moreover, they did not actually carry out the IC calculation for NES, instead they used the IC wave functions of Neodymium chloride given by Wybourne<sup>98</sup> to calculate the crystal field levels of NES. In fact, with the crystal field parameters given by Gruber and Satten and the correct IC wave functions of NES obtained from direct IC calculation we found that the predicted crystal field levels deviate from the values calculated by Gruber and Satten and also from the experimental values (see table III.1.5), the calculated g-values ( $g_{\parallel} = 3.559$ ,  $g_{\perp} = 2.15$ ) do not agree well with the observed values for the concentrated crystal and the calculated magnetic

susceptibilities at different temperatures, also deviate significantly from the experimental values.

In the back-drop of discrepancies mentioned above we have reinvestigated the problem rigorously by carrying out the actual IC calculation and using different J-mixing of  $^4I_{11/2}$ ,  $^4I_{13/2}$  and  $^4I_{15/2}$  with  $^4I_{9/2}$ . Attempts are then made to evaluate a unique set of parameters that will make the theory consistent with the e.p.r., optical absorption and magnetic susceptibility experiments simultaneously. A consistent interpretation of observed g-values, optical and magnetic susceptibility results in terms of a unique set of parameters has been possible only after we introduce a very small covalency reduction of the orbital angular momentum which effectively lowers the g-values and susceptibilities without altering the crystal field levels in the frame work of our theory. Indeed, a very good fit of all the above-mentioned experimental data has been achieved with a single set of parameters by introducing covalency reduction factors for the orbital moment very slightly less than unity into the present theory.

### III.1.2. CRYSTALLOGRAPHIC BACKGROUND OF RARE-EARTH ETHYL SULPHATES

Lanthanide ethyl sulphates,  $\text{Ln}(\text{C}_2\text{H}_5\text{SO}_4)_3 \cdot 9\text{H}_2\text{O}$ , whose X-ray crystallography was investigated by Ketelaar<sup>99</sup> (see Fig. III.1) and more

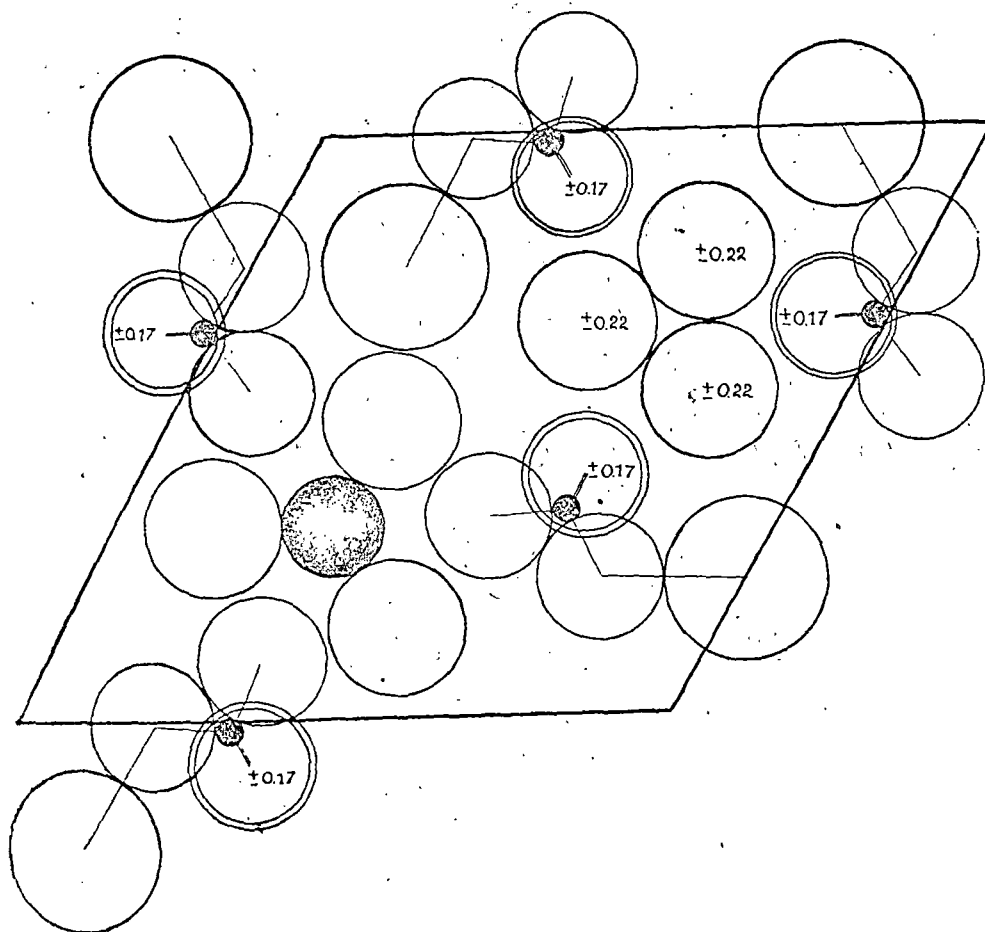


Fig. III.1.1. Projection of the lower half of the elementary cell on a plane at right angles with the  $c$ -axis on  $1/4$  of its height. The numbers indicate the distance to the plane of projection in fractions of the elementary period.  
 $S = \bullet$ ,  $Ce = \bullet$ ,  $O = \circ$ ,  $H_2O = \circ$ ,  $C_2H_5 = \circ$ . (The diameter of the various circles represents on scale the size of the atoms).

recently by Fitzwater and Rundle<sup>100</sup>. They studied the crystallographic structure of Pr, Er and Y. The latter workers show that all heavy atoms are found in the space group  $P6_3/m$  and that probably the hydrogen positions also conform to this space group. The point symmetry at the lanthanide ion is  $C_{3h}$ . This ion has nine water molecules as nearest neighbours; six form a triangular prism with three above and three below the mirror plane containing the other three water oxygens and the lanthanide ion (Fig. III.1.2). In Erbium compound the Er-O distances to the prism are 0.237 nm, and the remaining three distances are 0.252 nm. If all but the nearest oxygen positions are neglected, the symmetry about the lanthanide ion is almost  $D_{3h}$ . This structure has a vertical threefold axis of symmetry; if the structure were exactly  $D_{3h}$  there would also be both a vertical and horizontal plane of reflection symmetry. The compounds are isomorphous throughout the group from  $La^{3+}$  to  $Lu^{3+}$  and also  $Y^{3+}$ .

### III.1.3. METHOD OF CALCULATION

The  $Nd^{3+}$ -ion in the ethyl sulphate lattice is under a crystal field of hexagonal symmetry. Using the central field approximation the effective Hamiltonian of  $Nd^{3+}$ -ion in the crystal is given by

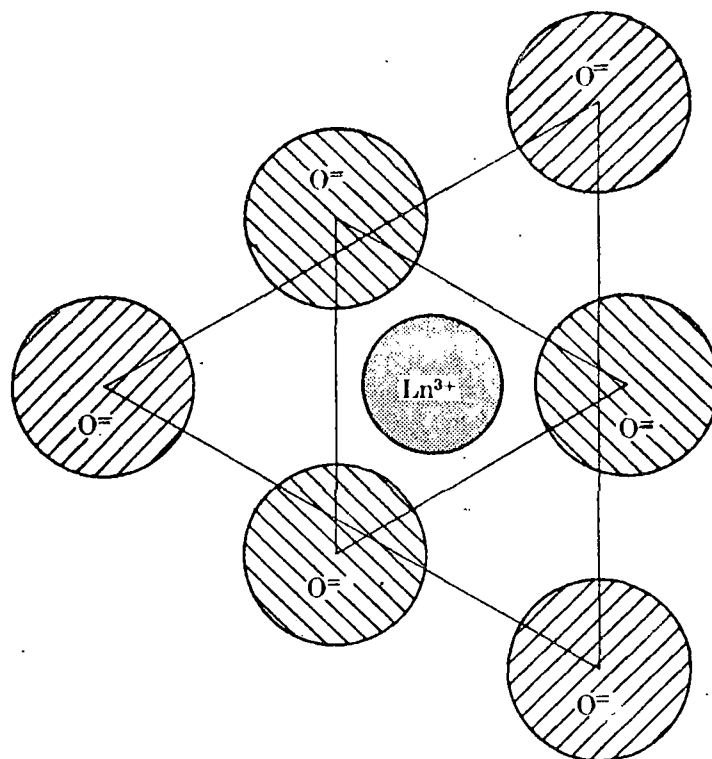


Fig. III.1.2. Arrangement of the double triangular prism of water oxygen ions in the lanthanide ethylsulphates, in a plan view as seen along the crystallographic  $c$ -axis. In  $(R, \theta, \phi)$  coordinates, the  $\text{Ln}^{3+}$  ion is at the origin; there are three  $\text{O}^{2-}$  ions in the same plane at  $(0.252 \text{ nm}, \pi/2, \phi = (2n+1)\pi/3)$ , and six  $\text{O}^{2-}$  ions (above and below) at  $(0.237 \text{ nm}, \theta, \phi = 2n\pi/3)$  and  $(0.237 \text{ nm}, \pi-\theta, \phi = 2n\pi/3)$  with  $\theta$  approximately  $40^\circ$ . The values of  $R$ ,  $\theta$  vary slightly with the lanthanide ion; the values of  $R$  given are for  $\text{Er}^{3+}$ . The radii of the circles denoting ions are drawn on about half scale relative to the inter-ionic distances.

$$\mathcal{H}_{\text{eff}} = H_r^{ij} + H_{\text{SO}} + H_C = \sum_{i < j} \frac{e^2}{r_{ij}} + \sum_i \zeta_i \cdot s_i + H_C$$

Using the intermediate coupling scheme we first diagonalise the matrix of  $H_r^{ij} + H_{\text{SO}}$  constructed in a basis of states represented by  $|U \circ \text{SLJM}\rangle$ , where the symbol  $\circ$  within the ket notation has been discussed in chapter II. The crystal field interaction,  $H_C$  is then treated as a perturbation over the resulting states which are actually the intermediate coupling wave functions.

Finally we apply Zeeman perturbation caused by an external magnetic field  $\mathcal{H}$  along and perpendicular to the symmetry axis of the ion in the form  $\beta \mathcal{H} (k_{\parallel} L_Z + 2S_Z)$  and  $\beta \mathcal{H} (k_{\perp} L_X + 2S_X)$  respectively where the covalency effect on the orbital angular momentum is introduced by associating the reduction factors  $k_{\parallel}$  and  $k_{\perp}$  with  $L_Z$  and  $L_X$  respectively. This way of introducing covalency reduction of orbital moment into the theory has been discussed earlier (chapter II). We ultimately obtain the principal g-values ( $g_{\parallel}$  and  $g_{\perp}$ ) and principal magnetic susceptibilities ( $K_{\parallel}$  and  $K_{\perp}$ ) of  $\text{Nd}^{3+}$ -ion.

#### III.1.4. INTERMEDIATE COUPLING WAVE FUNCTIONS

The diagonalisation of the matrix of  $H_r^{ij} + H_{\text{SO}}$  yields what are known as intermediate coupling wave-functions and their eigenvalues. For this we need the matrix elements of

$H_r^{ij}$  and  $H_{SO}$  both. The spin-orbit matrix element for  $4f^3$  configuration has been calculated by Judd and Loudon<sup>80</sup>. This can also be calculated by the general formula (II.8.1) given in chapter II along with the use of the tables of c.f.p. given by Nielson and Koster. The method of calculation of the matrix elements of electrostatic interaction  $H_r^{ij}$  has been described in chapter II. Gruber and Satten, in order to fit the 'free-ion' spectrum, deduced the values of the electrostatic parameters  $F_2 = 331.33 \text{ cm}^{-1}$ ,  $F_4 = 47.956 \text{ cm}^{-1}$ ,  $F_6 = 5.313 \text{ cm}^{-1}$  and SO coupling parameter  $\zeta = 880.11 \text{ cm}^{-1}$  for NES from those of  $\text{NdCl}_3$  following a procedure developed by Wong<sup>101</sup> without carrying out the IC calculation. We have used the same values for the parameters to calculate the numerical values of the IC matrix elements. The matrix of  $H_r^{ij} + H_{SO}$  constructed thus in a basis of states  $|U, S, L, J, M\rangle$  reduces to block form and each block corresponds to a particular value of  $J$ .

However, we need to consider only the four block matrices corresponding to  $J = 9/2, 11/2, 13/2$  and  $15/2$  in our calculation and the results for other values of  $J$  are not needed since the energy levels corresponding to other values of  $J$  are too high (more than  $10,000 \text{ cm}^{-1}$ ) to be included in the calculation of different  $J$ -mixing under the crystal field and of magnetic susceptibilities. It is to be noted that we need only the following four lowest wave functions and their corresponding energies in our subsequent calculation :

$$\begin{aligned} \Psi_1 = & 0.0031 |^4F_{9/2}\rangle - 0.0170 |^2G_{9/2}(20)\rangle + 0.0151 |^2G_{9/2}(21)\rangle \\ & + 0.0076 |^4G_{9/2}\rangle + 0.0577 |^2H_{9/2}(11)\rangle - 0.1636 |^2H_{9/2}(21)\rangle \\ & + 0.9845 |^4I_{9/2}\rangle \end{aligned}$$

with energy  $E_{\Psi_1}^{(0)} = 0$  (zero of the energy scale is taken at  $E_{\Psi_1}^{(0)}$ ),

$$\begin{aligned} \Psi_2 = & 0.0071 |^4G_{11/2}\rangle + 0.0367 |^2H_{11/2}(11)\rangle - 0.0945 |^2H_{11/2}(21)\rangle \\ & - 0.0151 |^2I_{11/2}\rangle + 0.9947 |^4I_{11/2}\rangle \end{aligned}$$

with energy  $E_{\Psi_2}^{(0)} = 1867.66 \text{ cm}^{-1}$ ,

$$\Psi_3 = -0.0231 |^2I_{13/2}\rangle + 0.0644 |^2K_{13/2}\rangle + 0.9977 |^4I_{13/2}\rangle$$

with energy  $E_{\Psi_3}^{(0)} = 3856.16 \text{ cm}^{-1}$ ,

$$\Psi_4 = 0.9930 |^4I_{15/2}\rangle + 0.1174 |^2K_{15/2}\rangle - 0.0090 |^4I_{15/2}\rangle$$

with energy  $E_{\Psi_4}^{(0)} = 5921.36 \text{ cm}^{-1}$ .

### III.1.5. CRYSTAL FIELD ENERGY LEVELS

For our purpose we actually need to calculate the crystal field effect only on the lowest intermediate coupling wave function  $\Psi_1$ . The effect of the crystal field is obtained by first diagonalising the matrix of  $H_c$  constructed in a basis of 10 states represented by  $|\Psi_1^{J_Z}\rangle$  where  $J_Z = \pm 9/2, \pm 7/2, \pm 5/2, \pm 3/2$  and  $\pm 1/2$ . This will give the first order correc-

tion to the energy of  $\Psi_1$  yielding a splitting of  $\Psi_1$  into five doublets and the correct zeroth order states for each component of the five doublets. The first order correction of the state is obtained by using the perturbation formula which involves the mixing of each of the aforesaid correct zeroth order state having  $J = 9/2$  with the states belonging to  $\Psi_2$ ,  $\Psi_3$  and  $\Psi_4$  having  $J$ -values equal to  $11/2$ ,  $13/2$  and  $15/2$  respectively. Thus the different  $J$ -mixing under the crystal field is obtained from the first order correction to the states.

The  $\text{Nd}^{3+}$  ion in ethyl sulphate lattice is under a crystal field of  $C_{3h}$  symmetry. However, as pointed out by Wybourne<sup>102</sup> and Abragam and Bleaney<sup>103</sup> we can also safely replace  $C_{3h}$  symmetry by a  $D_{3h}$  symmetry for the sake of calculation and indeed this has been the usual practice in treating the rare-earth ethyl sulphate ions. The CF interaction  $H_c$  assuming  $D_{3h}$  symmetry is given by

$$H_c = A_{20}U_o^{(2)} + A_{40}U_o^{(4)} + A_{60}U_o^{(6)} + A_{66}(U_6^{(6)} + U_{-6}^{(6)})$$

The CF parameters  $A_{kq}$  are not the same as  $B_k^q$  which are obtained when Stevens operator equivalent method is used and they are related as shown in chapter II.

By extensive trial method we have obtained the following set of parameters :

$$A_{20} = 180 \text{ cm}^{-1}, A_{40} = -645 \text{ cm}^{-1}, A_{60} = -730 \text{ cm}^{-1}, A_{66} = 624 \text{ cm}^{-1}$$

and the corresponding  $B_k^q$  values are  $B_2^0 = 56.8 \text{ cm}^{-1}$ ,  $B_4^0 = -68.2 \text{ cm}^{-1}$ ,  $B_6^0 = -46.4 \text{ cm}^{-1}$ ,  $B_6^6 = 602.8 \text{ cm}^{-1}$ . Using these values of the parameters the diagonalisation of the matrix of  $H_c$  constructed in a basis of the ten states  $|\Psi_1 J_Z\rangle$  where  $J_Z = \pm 9/2, \pm 7/2, \pm 5/2, \pm 3/2, \pm 1/2$  yields the following zeroth order CF states comprising five doublets and the first-order energy correction

$$\left. \begin{aligned} \phi_1^{(0)} &= 0.9105 |\Psi_1 7/2\rangle + 0.4136 |\Psi_1^{-5/2}\rangle \\ \phi_{1'}^{(0)} &= 0.9105 |\Psi_1^{-7/2}\rangle + 0.4136 |\Psi_1 5/2\rangle \end{aligned} \right\} \epsilon_1^{(1)} = -183.19 \text{ cm}^{-1},$$

$$\left. \begin{aligned} \phi_2^{(0)} &= 0.7552 |\Psi_1 9/2\rangle + 0.6555 |\Psi_1^{-3/2}\rangle \\ \phi_{2'}^{(0)} &= 0.7552 |\Psi_1^{-9/2}\rangle + 0.6555 |\Psi_1 3/2\rangle \end{aligned} \right\} \epsilon_2^{(1)} = -21.46 \text{ cm}^{-1},$$

$$\left. \begin{aligned} \phi_3^{(0)} &= |\Psi_1 \frac{1}{2}\rangle \\ \phi_{3'}^{(0)} &= |\Psi_1 -\frac{1}{2}\rangle \end{aligned} \right\} \epsilon_3^{(1)} = -30.96 \text{ cm}^{-1},$$

$$\left. \begin{aligned} \phi_4^{(0)} &= -0.6555 |\Psi_1 9/2\rangle + 0.7552 |\Psi_1^{-3/2}\rangle \\ \phi_{4'}^{(0)} &= -0.6555 |\Psi_1^{-9/2}\rangle + 0.7552 |\Psi_1 3/2\rangle \end{aligned} \right\} \epsilon_4^{(1)} = 125.18 \text{ cm}^{-1},$$

$$\left. \begin{aligned} \phi_5^{(0)} &= -0.4136 |\Psi_1 7/2\rangle + 0.9105 |\Psi_1^{-5/2}\rangle \\ \phi_{5'}^{(0)} &= -0.4136 |\Psi_1^{-7/2}\rangle + 0.9105 |\Psi_1 5/2\rangle \end{aligned} \right\} \epsilon_5^{(1)} = 110.44 \text{ cm}^{-1}$$

Next, we take the effect of J-mixing. Remembering that  $E_{\Psi_1}^{(0)}$  is the zero of the energy scale, the state correct to first order due to J-mixing is given by

$$\phi_i = N \left[ \phi_i^{(0)} - \sum_{\Psi_t} \frac{\langle \Psi_t | H_c | \phi_i^{(0)} \rangle}{E_{\Psi_t}^{(0)}} |\Psi_t\rangle \right] \quad (\text{III.1.1})$$

where  $t = 2, 3, 4$  and  $N$  is the normalization factor so that

$\langle \phi_i | \phi_i \rangle = 1$  and the CF energy correct to second order is

$$\epsilon_i = \epsilon_i^{(1)} - \sum_t \frac{|\langle \Psi_t | H_C | \phi_i^{(0)} \rangle|^2}{E_{\Psi_t}^{(0)}} \quad (\text{III.1.2})$$

there exist selection rules for  $M_J$  (the crystal quantum number is conserved) which strongly reduce the number of matrix elements to be considered in sum in (III.1.1) and (III.1.2).

The above crystal field states forming five doublets and originating from the lowest intermediate coupling wave function  $\Psi_1$  comprise the lowest group of levels originating from  $\Psi_2$ .

### III.1.6. COVALENCY REDUCTION OF ANGULAR MOMENTUM

We find that unless a reduction of the orbital momentum matrices is assumed presumably due to the covalency effect implying motion of the magnetic electrons in molecular orbitals, it becomes impossible to achieve a good fit to the  $g$ -values and magnetic susceptibilities. It has been discussed in chapter II that the matrix elements of  $L$  that occur in the calculation of  $g$ -values and magnetic susceptibilities are of the type

$$\langle SLJM | L_\alpha | S' L' J' M' \rangle \quad (\text{III.1.3})$$

where

$$\alpha \equiv x, y, z$$

in which the states refer to the whole atom built up from the individual electron state which are not pure f states but slightly modified due to covalency effect. It has also been discussed in chapter II that the effect of covalency on such matrix element will be to reduce the operator  $L_\alpha$  to  $k_\alpha L_\alpha$  and then calculate the matrix element of  $k_\alpha L_\alpha$  between the atomic states built up from pure f electronic states. The  $k_\alpha$  is the orbital reduction factor. Further it was shown in chapter II that in case of uniaxial symmetry we will have only two covalency reduction factors  $k_{\parallel}$  ( $= k_z$ ) and  $k_{\perp}$  ( $= k_x$  or  $k_y$ ). In the present theory the orbital reduction factors  $k_{\parallel}$  and  $k_{\perp}$  will be treated as two additional parameters to be evaluated from experiment.

### III.1.7. CALCULATION OF g-VALUES

For the calculation of the principal g-values one is interested only in the lowest doublet ( $\phi_1, \phi_1'$ ) in the CF level pattern. With the introduction of covalency reduction factors for the orbital momentum the expressions for the g-values are

$$g_{\parallel} = g_z = \left| \langle \phi_1 | k_{\parallel} L_z + 2S_z | \phi_1 \rangle - \langle \phi_1' | k_{\parallel} L_z + 2S_z | \phi_1' \rangle \right| ,$$

$$g_{\perp} = g_x = g_y = 2 \left| \langle \phi_1 | k_{\perp} L_x + 2S_x | \phi_1' \rangle \right| = 2 \left| \langle \phi_1 | k_{\perp} L_y + 2S_y | \phi_1' \rangle \right|$$

### III.1.8. CALCULATION OF SUSCEPTIBILITY

A significant contribution to the magnetic susceptibility comes from only the lowest group of ten CF states  $\phi_1$  forming five doublets. The general expression for the ionic paramagnetic susceptibility is obtained by the same way as described in chapter II.

### III.1.9. RESULTS AND DISCUSSION

The values of the parameters used in the theory are :  
 $F_2 = 331.33 \text{ cm}^{-1}$ ,  $F_4 = 47.956 \text{ cm}^{-1}$ ,  $F_6 = 5.313 \text{ cm}^{-1}$ ,  $\zeta = 880.11 \text{ cm}^{-1}$ ,  $B_2^0 = 56.8 \text{ cm}^{-1}$ ,  $B_4^0 = -68.2 \text{ cm}^{-1}$ ,  $B_6^0 = -46.4 \text{ cm}^{-1}$ ,  $B_6^6 = 602.8 \text{ cm}^{-1}$ ,  $k_{\parallel} = 0.987$ ,  $k_{\perp} = 0.997$ . The values of the crystal field energy levels, g-values ( $g_{\parallel}$  and  $g_{\perp}$ ) and magnetic susceptibility values  $K_{\parallel}$  and  $K_{\perp}$  at different temperatures of  $\text{Nd}^{3+}$  ion in NES calculated with the parameters mentioned above are shown in the tables III.1.5 - III.1.7. The symbols  $_{\parallel}$  and  $_{\perp}$  are used as suffix to indicate the quantities along the parallel and perpendicular to the symmetry axis of the ion. These tables also show the experimental values to facilitate comparison of the theory with the experiment.

Before we start interpreting the experimental results with the theory presented here we make a brief survey of the experimental results which are of interest to us. The principal

magnetic susceptibilities  $K_{\parallel}$  and  $K_{\perp}$  of  $\text{Nd}^{3+}$ -ion in the undiluted NES are available at different temperatures ranging from 14K to 291K from the works of Van den Handel and Hupse<sup>104</sup> (see table III.1.7). From the optical absorption experiment at 77K on undiluted NES Gruber and Satten gave the details of the crystal field energy levels into which the ground  $^4I_{9/2}$  level of the free ion splits (see table III.1.5). However, the resonance g-values that are available in the literature for the undiluted NES appear to be a little confusing. A magnetic resonance value  $g_{\parallel} = 3.61$  and  $g_{\perp} = 2.05$  for undiluted NES were quoted by Elliott and Stevens<sup>3</sup>, although the source was not mentioned. For NES which was diluted 200:1 with La-ethyl sulphate Bleaney et al.<sup>91</sup> gave the following g-values for their e.p.r experiment at 20K :  $g_{\parallel} = 3.53$ ,  $g_{\perp} = 2.08$  . They further reported that for concentrated NES similar values were obtained, of course with a less degree of accuracy. It is not clear whether these 'similar' values which refer to the concentrated crystal were identical with those for the diluted crystal. On the other hand, very recently Fisher et al.<sup>97</sup> from magneto-thermodynamic studies at extremely low temperature (about 4K) found the accurate g-values of the concentrated crystals to be  $g_{\parallel} = 3.594$  and  $g_{\perp} = 2.039$  which is very close to the values quoted by Elliott and Stevens<sup>3</sup> .

Without actually carrying out the diagonalisation of IC matrices of NES, Gruber and Satten evaluated the electrostatic parameters  $F_2$ ,  $F_4$ ,  $F_6$  and SO parameter  $\zeta$  in the new system of NES from those of  $\text{NdCl}_3$  following a method developed by Wong<sup>105</sup> in which a Taylor series expansion of the energy values was used. Wong also indicated that Taylor series expansion method can also be applied to find the wave function in the new system. Gruber and Satten did not make any attempt to find the wave function of NES from those of  $\text{NdCl}_3$  and instead he used those of  $\text{NdCl}_3$  for further calculation of crystal field splitting. We have used the values of the above parameters to calculate the IC wave functions by diagonalisation of IC matrices and the corresponding energy values calculated with these values of  $F_2$ ,  $F_4$ ,  $F_6$  and  $\zeta$  are presented in tables III.1.1 - III.1.4. As expected, the 'free-ion' levels of NES that are obtained thus from actual diagonalisation of IC matrices are in exact agreement with those obtained by Gruber and Satten using Wong's procedure. However, the IC wave functions for NES obtained from diagonalisation of the IC matrices are slightly different from those of  $\text{NdCl}_3$  since the parameters in the two systems are slightly different.

The crystal field parameters  $A_{20}$ ,  $A_{40}$ ,  $A_{60}$  and  $A_{66}$  are then chosen by an exhaustive trial method and so as to

fit the theory with the observed crystal field spectra as close as possible. The parameters giving the best fit are shown in table III.1.5, the predicted and observed crystal field levels agree almost exactly (within a mean deviation of  $1 \text{ cm}^{-1}$  only). The crystal field parameters in our theory are somewhat different from those of Gruber and Satten. Gruber and Satten evaluated them by fitting the predicted levels obtained by using IC wave functions of  $\text{NdCl}_3$  instead of NES with the observed levels within a mean deviation of  $4 \text{ cm}^{-1}$ . However, with the correct IC wave functions of NES their parameters predict the crystal field levels which deviate considerably (about  $12 \text{ cm}^{-1}$  in some cases) from the observed spectra (see table III.1.5).

Having found the 'free-ion' and crystal field parameters which fit the predicted and observed spectra so nicely, it is expected that they should also faithfully reproduce the observed g-values and magnetic susceptibilities. On actual calculation with the crystal field parameters obtained by us and with the correct IC wave functions of NES without taking covalency effect into consideration (i.e.  $k_{\parallel} = k_{\perp} = 1$ ) g-values come out to be  $g_{\parallel} = 3.674$ ,  $g_{\perp} = 2.052$  as against the recent values determined by Fisher et al.<sup>97</sup>  $g_{\parallel} = 3.594$ ,  $g_{\perp} = 2.039$ . Moreover, both the principal susceptibilities  $K_{\parallel}$  and  $K_{\perp}$  are found to be larger than the experimental values.

However, if we introduce a very small covalency effect on the orbital angular momentum operator by using the covalency reduction factors  $k_{\parallel} = 0.987$  and  $k_{\perp} = 0.997$ , we arrive at a good fitting of not only the  $g$ -values but also the principal magnetic susceptibilities, with the same set of parameters that explained the optical spectra with remarkable success. The predicted  $g$ -values are  $g_{\parallel} = 3.596$ ,  $g_{\perp} = 2.041$  in excellent agreement with the observed values. Also the theory is found to fit the magnetic data almost exactly (within 0.37%) at the lowest temperature of measurement (14K). At room temperature the theory is found to agree with the magnetic data within 1.4% and the maximum deviation that occurs at some intermediate temperature is found to be about 6% of the observed values.

The values of  $k_{\parallel}$  and  $k_{\perp}$  indicate that the covalency effect is very small as expected in the case of rare-earth ions. The covalency should also affect all parameters. In fact, Ellis and Newman<sup>106</sup> carried out an ab initio calculation for the theoretical estimates of the contribution from various factors including covalency to the CF parameters. However, in a theory using adjustable parameters to be evaluated from experiment, the values of the parameters deduced from experiment will automatically include the effect of covalency.

Some of the CF parameters given by Gruber and Satten have been slightly modified in the present investigation to

improve the fitting of the theory with the experiments on  $g$ -values and magnetic susceptibilities. In the present work  $B_4^0$  remains unchanged at the value given by Gruber and Satten,  $B_2^0$  changes from 58.4 to 56.8  $\text{cm}^{-1}$ ;  $B_6^0$  from -42.7 to -46.4  $\text{cm}^{-1}$  and  $B_6^6$  from 595 to 602.8  $\text{cm}^{-1}$ . Since these changes are small, the present values of the parameters are expected not to disturb seriously the whole crystal field spectra. In fact, with the present CF parameters energy values of the CF components of the ground term have already been determined in the course of our calculation on the magnetic properties. They are shown in table III.1.7 along with the experimental results. The table III.1.5 shows that the small changes in the values of some of the CF parameters from those of Gruber and Satten in no way disturb the fitting of the CF spectra of the ground group of levels. We expect that excited CF levels will also not be seriously affected owing to the small changes that have been made in the values of the CF parameters given by Gruber and Satten.

In the present investigation we have considered that the crystal field parameters are independent of temperature as otherwise the solution of the parameters from the available experimental data will be nonunique. In the iron group the anisotropic component of the ligand field is found to vary with temperature in many cases<sup>107-109</sup>. Variation of the

crystal field parameters in our case, if any, must be small as found from the nature of agreement of the theory with the magnetic data and may account for the slight discrepancy that still persists at some temperature. There may also exist a very slight distortion from the  $C_{3h}$  symmetry to  $C_{3v}$  symmetry as was postulated by Elliott and Stevens<sup>110</sup> in the case of Ce-ethylsulphate. However, for further refinement of the theory a redetermination of the magnetic data with the presently available refined technique and purer samples is considered to be imperative. The magnetic measurements were done long ago and an accurate redetermination will ascertain whether the small discrepancy that still persists while interpreting the magnetic data with the present theory is really of any significance.

Numerical computation was done with the help of the computer (Burroughs 6700) at the Regional Computer Centre, Calcutta as far as practicable leaving hand calculation to the minimum.

Table III.1.1

IC wave functions and corresponding energies of Nd<sup>3+</sup> for J = 9/2<sup>(a)</sup>, (b)

Energy	14645.51	20877.77	47738.63	19375.66	32560.43	12475.50	0
Eigen Vectors							
<sup>4</sup> F	0.8703	0.2766	0.0156	-0.1959	0.0037	-0.3570	0.0031
<sup>2</sup> G <sub>20</sub>	-0.1325	0.6020	0.6436	-0.3026	-0.0159	0.3372	-0.0170
<sup>2</sup> G <sub>21</sub>	0.0909	-0.4911	0.7598	0.2869	-0.1000	-0.2842	0.0151
<sup>4</sup> G	-0.0339	0.5190	-0.0218	0.8394	0.0655	-0.1415	0.0076
<sup>2</sup> H <sub>11</sub>	-0.1570	0.0045	0.0814	-0.1296	0.9283	-0.2947	0.0577
<sup>2</sup> H <sub>21</sub>	0.4306	-0.2234	0.0341	0.2552	0.3517	0.7403	-0.1636
<sup>4</sup> I	0.0746	-0.0244	0.0004	0.0345	0.0048	0.1527	0.9845

(a)  $F_2 = 331.33 \text{ cm}^{-1}$ ,  $F_4 = 47.956 \text{ cm}^{-1}$ ,  $F_6 = 5.313 \text{ cm}^{-1}$ ,  $\zeta = 880.11 \text{ cm}^{-1}$

(b) Energy of IC wave functions are given at the top of the columns. For the IC wave function of a particular energy the co-efficient of each constituent <sup>2S+1</sup>L<sub>UV</sub> state shown in the first column is given by the corresponding entry in the column where this energy occurs.

Table III.1.2

IC wave functions and the corresponding energies of Nd<sup>3+</sup>  
for  $J = 11/2$  (a), (b)

	21432.40	33902.63	15770.0	28459.26	1867.66
Energy					
Eigen Vectors					
<sup>4</sup> G	0.9642	0.1128	-0.2308	-0.0661	0.0071
<sup>2</sup> H <sub>11</sub>	-0.2109	0.8372	-0.3746	-0.2362	0.0367
<sup>2</sup> H <sub>21</sub>	0.1598	0.4005	0.8910	-0.1059	-0.0945
<sup>2</sup> I	0.0101	0.3548	-0.0520	0.9333	-0.0151
<sup>4</sup> I	0.0162	0.0117	0.0994	0.1700	0.9947

(a) Parameters same as Table III.1.1 .

(b) Explanation of the table same as Table III.1.1 .

Table III.1.3

IC wave functions and the corresponding energies of  $\text{Nd}^{3+}$   
for  $J = 13/2$  (a), (b)

Energy	29770.80	3856.16	18040.81
Eigen Vectors			
$^2\text{I}$	0.9948	-0.0231	-0.0995
$^4\text{I}$	0.0166	0.9977	-0.0664
$^2\text{K}$	0.1008	0.0644	0.9928

(a) Parameters same as Table III.1.1 .

(b) Explanation of the table same as Table III.1.1 .

Table III.1.4

IC wave functions and the corresponding energies of  $\text{Nd}^{3+}$   
for  $J = 15/2$  <sup>(a), (b)</sup> .

Energy	5921.36	20777.68	29233.16
Eigen Vectors			
$^4\text{I}$	0.9930	-0.1166	-0.0161
$^2\text{K}$	0.1174	0.9705	0.2107
$^2\text{L}$	-0.0090	-0.2111	0.9774

(a) Parameters same as Table III.1.1

(b) Explanation of the table same as Table III.1.1 .

Table III.1.5

Comparison of the calculated crystal field energy levels with the experimentally observed levels<sup>96</sup>.

Crystalline Stark Component	Experimental energy level	Predicted energy level considering second order correction with present set of parameters: $B_2^0 = 56.8 \text{ cm}^{-1}$ , $B_4^0 = -68.2 \text{ cm}^{-1}$ , $B_6^0 = -46.4 \text{ cm}^{-1}$ , $B_6^6 = 602.8 \text{ cm}^{-1}$	Predicted energy level considering second order correction with the Gru- ber's set of parameters: $B_2^0 = 58.4 \text{ cm}^{-1}$ , $B_4^0 = -68.2 \text{ cm}^{-1}$ $B_6^0 = -42.7 \text{ cm}^{-1}$ , $B_6^6 = 595 \text{ cm}^{-1}$
<u>+5/2</u>	0	0	0
<u>+3/2</u>	149	149	142
<u>+1/2</u>	154	155	154
<u>+5/2</u>	279	279	268
<u>+3/2</u>	311	310	299

Table III.1.6

Comparison between calculated and experimental g-values  
(Covalency reduction factors  $k_{\parallel} = 0.989$ ,  $k_{\perp} = 0.998$ ).

Calculated	Experimental
$g_{\parallel} = 3.608$	$g_{\parallel} = 3.594^{97}$ , $g_{\parallel} = 3.61^3$
$g_{\perp} = 2.044$	$g_{\perp} = 2.039^{97}$ , $g_{\perp} = 2.05^3$

Table III.1.7

Comparison of calculated values  $K_{\parallel}$ ,  $K_{\perp}$  with the experimentally observed values.

Temp. (T) °K	Predicted results		Experimental results <sup>104</sup>	
	$K_{\parallel} \times 10^6$ , c.g.s. e.m.u.	$K_{\perp} \times 10^6$ , c.g.s. e.m.u.	$K_{\parallel} \times 10^6$ , c.g.s. e.m.u.	$K_{\perp} \times 10^6$ , c.g.s. e.m.u.
14.27	90525.34	34619.00	90257.08	34623.54
17.70	73949.83	29296.33	72873.73	29490.34
20.34	64998.27	26422.75	64625.1	26572.67
64.6	23113.42	13455.66	21616.72	12877.31
71.0	21225.60	12906.89	20246.49	12270.60
77.7	19553.10	12402.42	18644.50	11895.67
139.3	11264.58	9100.89	10682.24	8643.96
216.8	7261.65	6560.05	7103.31	6455.70
226.8	6938.90	6319.62	6905.62	6278.46
249.8	6293.15	5822.57	6292.09	5787.63
287.5	5456.17	5147.12	5474.05	5119.57
291.5	5380.00	5083.94	5378.61	4996.86

### III.2. INTERPRETATION OF THE OPTICAL, MAGNETIC AND THERMAL BEHAVIOURS OF THULIUM ETHYL SULPHATE

#### III.2.1. INTRODUCTION

The present section aims at a consistent interpretation of the optical absorption spectra, magnetic heat capacity and magnetic susceptibility of Thulium ethyl sulphate (Tm.ES.) with a single set of parameters.<sup>110a</sup> From the results of optical absorption experiment on concentrated Tm.ES. Gruber and Conway<sup>111-112</sup> first determined a set of electrostatic (ES), spin-orbit (SO) and crystal field (CF) parameters that accounted for the observed levels which were limited in number. Wong and Richman<sup>113</sup> also did the spectroscopic investigation on the diluted crystals of Tm.ES. and gave a different set of crystal field parameters. Gerstein et al.<sup>114</sup> measured the magnetic susceptibility and magnetic heat capacity of concentrated Tm.ES. at different temperatures and tried to fit their experimental data theoretically with the parameters obtained from Wong and Richman<sup>113</sup> and Gruber and Conway<sup>112</sup>. Gerstein et al found that Wong's crystal field parameters which actually referred to the diluted crystals of  $\text{Tm}^{3+}$  in  $\text{La}(\text{C}_2\text{H}_5\text{SO}_4)_3 \cdot 9\text{H}_2\text{O}$  gave a better fitting of the magnetic susceptibility and magnetic heat capacity data than the parameters given by Gruber et al for undiluted crystals of Tm.ES.

In a later investigation more levels were observed by Krupke and Gruber<sup>115</sup> in optical absorption experiment on undiluted crystal of Tm.ES. But all the crystal field calculations on Tm.ES. primarily meant to fit the optical data were restricted to first order perturbation calculations (i.e., neglecting J-mixing among the states). But in the present work we have carried out the diagonalisation of the matrix of spin-orbit (SO), electrostatic (ES) and the crystal field (CF) interaction of Tm.ES. considered together, the matrix being constructed in a basis of all states of  $Tm^{3+}$  ion in the  $4f^{12}$  configuration. Thus the full J-mixing was taken into account and which is the most realistic approach. Finally these results were used to obtain the magnetic susceptibility and magnetic heat capacity data. We find that the set of parameters given by Krupke and Gruber<sup>115</sup> when used in our full J-mixing calculation, can fit very well the magnetic susceptibility, optical levels and the magnetic heat capacity data, though slight discrepancies arise in some optical levels which will be discussed later.

### III.2.2. SPECTRA OF Tm.ES.

The effective Hamiltonian of  $Tm^{3+}$  in Tm.ES. crystal having a  $D_{3h}$  symmetry is given by

$$\mathcal{H}_{\text{eff}} = \sum_{i < j} \frac{e^2}{r_{ij}} + \sum_i l_i \cdot s_i + A_{20} U_0^{(2)} + A_{40} U_0^{(4)} + A_{60} U_0^{(6)} \\
 + A_{66} (U_6^{(6)} + U_{-6}^{(6)})$$

where  $U_q^{(k)} = r^k Y_k^q$  is an irreducible tensor operator.  $A_{kq}$ 's are the crystal field parameters which are related with Stevens form  $B_k^q$ 's as shown in chapter II.

The matrix of the effective Hamiltonian  $\mathcal{H}_{\text{eff}}$  is constructed in a basis of states represented by  $|U^3SLJM\rangle$ . All states belonging to the different multiplet terms  ${}^3P_{FH}^1SDGI$  of  $Tm^{3+}$  have been taken into consideration for the representation of the above matrix and it turns out to be a  $91 \times 91$  matrix. The matrix elements of ES interaction for  $4f^2$  configuration expressed in terms of Slater-Condon parameters  $F_k$ 's have been tabulated by Nielson and Koster<sup>77</sup>. We used those for our  $f^{12}$  system since it will be exactly same. The SO matrix elements can be easily calculated by using the formula given by Elliott et al.<sup>89</sup> The SO matrix elements for  $f^2$  system have also been already calculated by Spedding<sup>79</sup>. We use these results of  $f^2$  in our  $f^{12}$  system by reversing the sign of each matrix element of the spin-orbit interaction. The matrix element of  $U_q^{(k)}$  was obtained by procedure described earlier (Chapter II), using tensor operator technique and thus the  $91 \times 91$  full matrix is set up. But due to the crystal symmetry, the whole matrix splits up into 2 matrices of dimension  $16 \times 16$

(crystal quantum number  $\bar{\mu} = \pm 2$ ), 3 matrices of dimension 14x14 (of which 2 matrices have  $\bar{\mu} = \pm 1$  and another  $\bar{\mu} = 3$ ) and one matrix of dimension 17x17 ( $\bar{\mu} = 0$ ).

A complete computer program was then made in which the CF matrix elements were automatically generated and then added up to spin-orbit and electrostatic contribution and after that 6 matrices were diagonalized individually by the same program. The program then invokes a second portion of the program which automatically calculates the susceptibilities and the magnetic heat capacity at different temperatures.

### III.2.3. CALCULATION OF SUSCEPTIBILITY

A significant contribution to the magnetic susceptibility of  $Tm^{3+}$  comes from only the lowest multiplet of  $^3H_6$ . It contains 13 crystal field states  $\phi_i$ 's of which 4 are doublets and 5 are singlets. The general expression for calculating the ionic susceptibility is given in chapter II. The 13 CF states are given in Appendix III.2 at the end of this section.

### III.2.4. CALCULATION OF MAGNETIC HEAT CAPACITY

The magnetic heat capacity of  $Tm.E.S.$  is theoretically obtained from

$$C_m = \frac{R}{Z^2} \left[ Z \sum_{m=1}^n \left( \frac{E_m^0}{kT} \right)^2 \exp \left( - \frac{E_m^0}{kT} \right) - \sum_{m=1}^n \frac{E_m^0}{kT} \exp \left( - \frac{E_m^0}{kT} \right) \right]$$

$E_m^O = W_m^O - W_1^O$  where  $W_1^O$  = Energy of lowest CF level. Here  $n = 13$  since for  $Tm^{3+}$  ion  $^3H_6$  is the ground term and it splits into 13 levels in a crystal field, where

$k$  = Boltzman constant,

$R = Nk$ ,

$T$  = Temperature.

We then calculate the magnetic heat capacity of  $Tm.E.S.$  at different temperatures using the energy values of the CF levels which give the best fit to the experimental crystal field energy levels and the magnetic susceptibility.

### III.2.5. RESULTS AND DISCUSSION

In our present calculation we have done an exhaustive trial method to see which set of parameters can give an overall good fitting. We found that Krupke and Gruber's set of parameters gave an overall good agreement. The parameters taken are as follows :

$$F_2 = 449.16 \text{ cm}^{-1}, F_4 = 64.57 \text{ cm}^{-1}, F_6 = 7.065 \text{ cm}^{-1},$$

$$\zeta = 2667.9 \text{ cm}^{-1}, B_2^O \langle r^2 \rangle = 135.3 \text{ cm}^{-1}, B_4^O \langle r^4 \rangle = -71.35 \text{ cm}^{-1},$$

$$B_6^O \langle r^6 \rangle = -28.8 \text{ cm}^{-1}, B_6^6 \langle r^6 \rangle = 428.1 \text{ cm}^{-1} .$$

Table III.2.1 shows the experimental crystal field levels and the theoretical levels obtained from the above exact calculation by using Krupke and Gruber's set of parameters. Fig. III.2.1 shows

the theoretical points and the experimental curves of  $K_{II}$  and  $K_I$  at different temperatures. Fig. III.2.2 shows the theoretical points and the experimental curve of  $C_m$  at different temperatures.

We find that Johnsen<sup>116</sup> and all the subsequent workers wrongly assigned the  $^3F_4$  level. In a recent work on  $Tm^{3+}$  in  $LaCl_3$  Gruber et al<sup>10</sup> obtained the  $^3H_4$  multiplet at about  $12624 \text{ cm}^{-1}$  (mean value) from the ground level. But in his works on  $Tm.E.S.$  which were done earlier it was wrongly interpreted that the  $^3F_4$  manifold lies at about  $12600 \text{ cm}^{-1}$  from the ground term. It now appears from our theoretical calculation that it is the  $^3H_4$  and not  $^3F_4$  which lies at  $12600 \text{ cm}^{-1}$  and  $^3F_4$  lies at  $6000 \text{ cm}^{-1}$ . The observed levels of  $Tm^{3+}$  in  $LaCl_3$  also confirm this. We also find that Krupke and Gruber's set of parameters can fit almost all the experimental optical levels with the theoretical levels except the  $^1I_6$  level. We also find that no new set of parameters can improve the  $^1I_6$  level without affecting the other levels like  $^1G_4$  and so on. This discrepancy in  $^1I_6$  may be due to the configuration mixing. Fig. III.2.1 shows that above 24K a good fit is obtained between the theoretical points and the experimental curve for  $K_{II}$ . Gerstein et al also could not fit this portion with Wong's parameters. They expressed doubt about the reliability of the absolute values of experimental data in this portion due to some experimental inaccuracies. The theoretical values

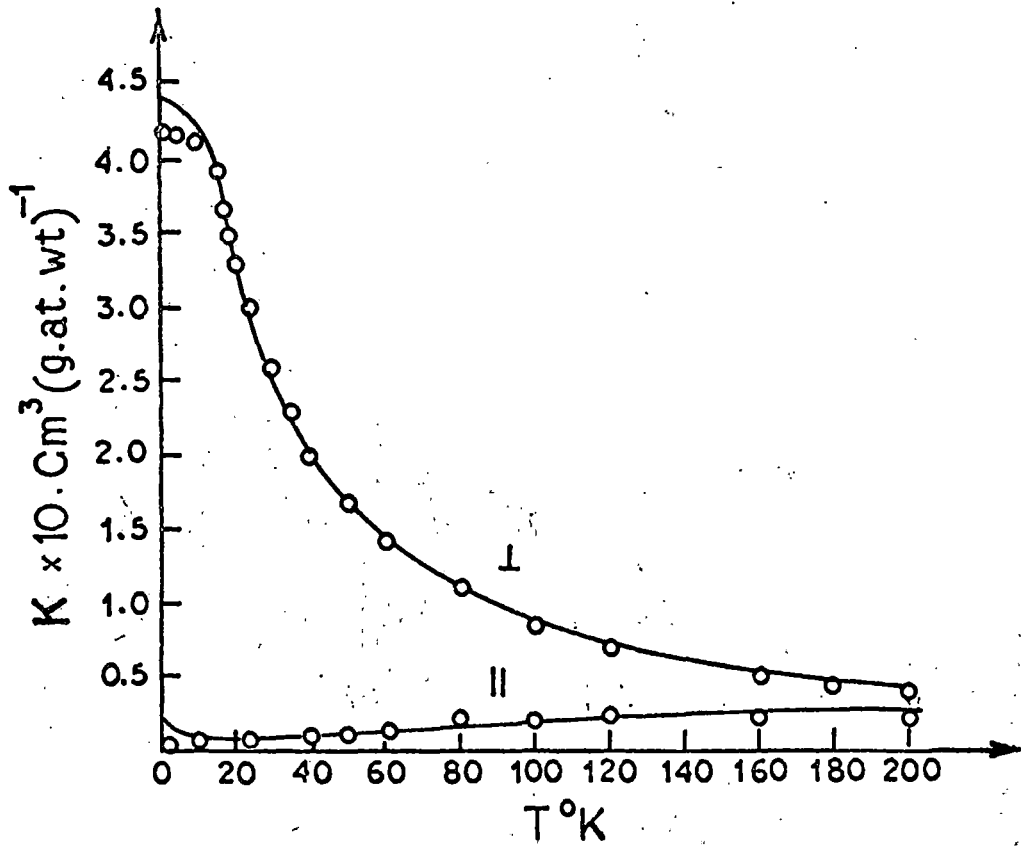


Fig. III.2.1.  $K_{II}$  and  $K_{I}$  of Tm ES.,  $\text{cm}^3 (\text{g}\cdot\text{at. wt})^{-1}$ .

○ Theoretical points.

— Experimental smoothed curve.

of  $K_1$  are very close to the experimental curve. From Fig. III.2.2 we find that there is a sharp rise of experimental curve of  $C_m$  values upto 16K and then a gradual decrease in the value upto 40K then again a gradual rise in the value upto 80K after that again a rapid fall occurs. Fig. III.2.2 also shows that the theoretical values do not fit well at low temperatures but at higher temperatures they are almost on the experimental curve.

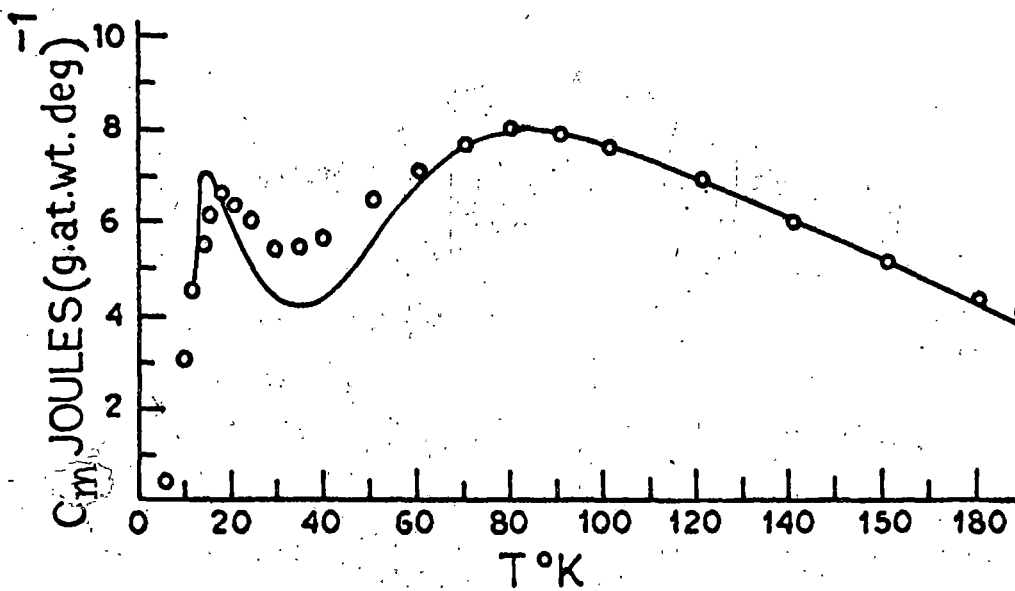


Fig. III.2.2.  $C_m$  of Tm.ES.,  $\text{J (g.at. wt. deg)}^{-1}$ .

○ Theoretical points.

— Experimental smoothed curve.

Table III.2.1

Comparison between experimental and theoretical values of crystal field splitting.

Terms	$\mu$	Experimental levels	Theoretical levels
${}^3H_6$	0	0	0
	+1	32	33
	+2	112	115
	3	176	165
	+1	201	207
	0	-	219
	0	-	224
	+2	277	278
	3	305	305
${}^3H_4$	0	-	12592
	3	-	12637
	+1	-	12672
	+2	-	12692
	3	-	12785
	+2	-	12820
${}^3F_3$	3	14407	14402
	+1	14466	14455
	+2	14486	14483
	3	14487	14493
${}^3F_2$	+2	15079	14966
	+1	15106	14983
${}^1G_4$	+2	21168	21120
	+1	21191	21138
	0	21255	20945
	+2	21279	21233
	3	21341	21276
	3	21379	21420
${}^1D_2$	+2	27906	27885
	+1	27977	27951
${}^1I_6$	+2	34844	33801
	3	34871	33825
	+2	34900	33854
${}^3P_0$	0	35442	35456
${}^3P_1$	0	36401	36304
	+1	36486	36385
${}^3P_2$	+2	38147	38166
	+1	38188	38200
	0	38312	38350

APPENDIX III.2.

CF wave functions and the energy values of the ground term ( $^3H_6$ ) of Thulium ethyl sulphate obtained from Krupke and Gruber's<sup>115</sup> set of parameters

$$\begin{aligned}
 \Phi_1 = & 0.1154 |^3H_6 6\rangle + 0.9820 |^3H_6 0\rangle + 0.1154 |^3H_6 -6\rangle \\
 & -0.0000 |^3H_5 0\rangle - 0.0025 |^3H_4 0\rangle - 0.0018 |^3F_4 0\rangle \\
 & -0.0000 |^3F_3 0\rangle + 0.0028 |^3F_2 0\rangle - 0.0021 |^3P_2 0\rangle \\
 & -0.0000 |^3P_1 0\rangle - 0.0009 |^3P_0 0\rangle + 0.0109 |^1I_6 6\rangle \\
 & + 0.0936 |^1I_6 0\rangle + 0.0109 |^1I_6 -6\rangle + 0.0009 |^1G_4 0\rangle \\
 & - 0.0017 |^1D_2 0\rangle + 0.0002 |^1S_0 0\rangle
 \end{aligned}
 \left. \vphantom{\Phi_1} \right\} W_1^{(0)} = 0$$
  

$$\begin{aligned}
 \Phi_2 = & 0.2858 |^3H_6 5\rangle + 0.9535 |^3H_6 -1\rangle - 0.0021 |^3H_5 5\rangle \\
 & - 0.0065 |^3H_5 -1\rangle - 0.0007 |^3H_4 -1\rangle + 0.0002 |^3F_4 -1\rangle \\
 & + 0.0032 |^3F_3 -1\rangle + 0.0007 |^3F_2 -1\rangle - 0.0021 |^3P_2 -1\rangle \\
 & - 0.0009 |^3P_1 -1\rangle + 0.0272 |^1I_6 5\rangle + 0.0910 |^1I_6 -1\rangle \\
 & + 0.0005 |^1G_4 -1\rangle - 0.0009 |^1D_2 -1\rangle
 \end{aligned}
 \left. \vphantom{\Phi_2} \right\} W_2^{(0)} = 33 \text{ cm}^{-1}$$

$$\Phi_2 = \left. \begin{array}{l} 0.2858 |^3H_6 -5\rangle + 0.9535 |^3H_6 1\rangle - 0.0021 |^3H_5 -5\rangle \\ -0.0065 |^3H_5 1\rangle - 0.0007 |^3H_4 1\rangle + 0.0002 |^3F_4 1\rangle \\ +0.0032 |^3F_3 1\rangle + 0.0007 |^3F_2 1\rangle - 0.0021 |^3P_2 1\rangle \\ -0.0009 |^3P_1 1\rangle + 0.0272 |^1I_6 5\rangle + 0.0910 |^1I_6 1\rangle \\ +0.0005 |^1G_4 1\rangle - 0.0009 |^1D_2 1\rangle \end{array} \right\} W_2^{(0)} = 33 \text{ cm}^{-1}$$

$$\Phi_3 = \left. \begin{array}{l} 0.8964 |^3H_6 2\rangle + 0.4327 |^3H_6 -4\rangle + 0.0058 |^3H_5 2\rangle \\ +0.0068 |^3H_5 -4\rangle + 0.0024 |^3H_4 2\rangle + 0.0013 |^3H_4 -4\rangle \\ +0.0015 |^3F_4 2\rangle - 0.0069 |^3F_4 -4\rangle - 0.0002 |^3F_3 2\rangle \\ -0.0027 |^3F_2 2\rangle - 0.0017 |^3P_2 2\rangle + 0.0859 |^1I_6 2\rangle \\ +0.0414 |^1I_6 -4\rangle - 0.0010 |^1G_4 2\rangle - 0.0031 |^1G_4 -4\rangle \\ +0.0005 |^1D_2 2\rangle \end{array} \right\} W_3^{(0)} = 115 \text{ cm}^{-1}$$

$$\Phi_3' = \left. \begin{array}{l} 0.8964 |^3H_6 -2\rangle + 0.4327 |^3H_6 4\rangle + 0.0058 |^3H_5 -2\rangle \\ +0.0068 |^3H_5 4\rangle + 0.0024 |^3H_4 -2\rangle + 0.0013 |^3H_4 4\rangle \\ +0.0015 |^3F_4 -2\rangle - 0.0069 |^3F_4 4\rangle - 0.0002 |^3F_3 -2\rangle \\ -0.0027 |^3F_2 -2\rangle - 0.0017 |^3P_2 -2\rangle + 0.0859 |^1I_6 -2\rangle \\ +0.0414 |^1I_6 4\rangle - 0.0010 |^1G_4 -2\rangle - 0.0031 |^1G_4 4\rangle \\ +0.0005 |^1D_2 -2\rangle \end{array} \right\} W_3^{(0)} = 115 \text{ cm}^{-1}$$

$$\Phi_4 = \left. \begin{array}{l} 0.7038 |^3H_6 3\rangle + 0.7038 |^3H_6 -3\rangle - 0.0033 |^3H_5 3\rangle \\ +0.0033 |^3H_5 -3\rangle + 0.0034 |^3H_4 3\rangle + 0.0034 |^3H_4 -3\rangle \\ -0.0023 |^3F_4 3\rangle - 0.0023 |^3F_4 -3\rangle + 0.0045 |^3F_3 3\rangle \\ -0.0045 |^3F_3 -3\rangle + 0.0676 |^1I_6 3\rangle + 0.0676 |^1I_6 -3\rangle \\ -0.0029 |^1G_4 3\rangle - 0.0029 |^1G_4 -3\rangle \end{array} \right\} W_4^{(0)} = 165 \text{ cm}^{-1}$$

$$\begin{aligned}
 \Phi_5 = & 0.9535 |^3H_6 5\rangle - 0.2857 |^3H_6 -1\rangle + 0.0020 |^3H_5 5\rangle \\
 & + 0.0099 |^3H_5 -1\rangle + 0.0024 |^3H_4 -1\rangle + 0.0079 |^3F_4 -1\rangle \\
 & + 0.0049 |^3F_3 -1\rangle + 0.0029 |^3F_2 -1\rangle + 0.0011 |^3P_2 -1\rangle \\
 & + 0.0009 |^3P_1 -1\rangle + 0.0913 |^1I_6 5\rangle - 0.0275 |^1I_6 -1\rangle \\
 & + 0.0012 |^1G_4 -1\rangle - 0.0008 |^1D_2 -1\rangle
 \end{aligned}
 \left. \vphantom{\Phi_5} \right\} W_5^{(0)} = 207 \text{ cm}^{-1}$$

$$\begin{aligned}
 \Phi_5' = & 0.9535 |^3H_6 -5\rangle - 0.2857 |^3H_6 1\rangle + 0.0020 |^3H_5 -5\rangle \\
 & + 0.0099 |^3H_5 1\rangle + 0.0024 |^3H_4 1\rangle + 0.0079 |^3F_4 1\rangle \\
 & + 0.0049 |^3F_3 1\rangle + 0.0029 |^3F_2 1\rangle + 0.0011 |^3P_2 1\rangle \\
 & + 0.0009 |^3P_1 1\rangle + 0.0913 |^1I_6 -5\rangle - 0.0275 |^1I_6 1\rangle \\
 & + 0.0012 |^1G_4 1\rangle - 0.0008 |^1D_2 1\rangle
 \end{aligned}
 \left. \vphantom{\Phi_5'} \right\} W_5^{(0)} = 207 \text{ cm}^{-1}$$

$$\begin{aligned}
 \Phi_6 = & -0.7039 |^3H_6 6\rangle - 0.0000 |^3H_6 0\rangle + 0.7039 |^3H_6 -6\rangle \\
 & - 0.0068 |^3H_5 0\rangle + 0.0000 |^3H_4 0\rangle + 0.0000 |^3F_4 0\rangle \\
 & - 0.0079 |^3F_3 0\rangle + 0.0000 |^3F_2 0\rangle + 0.0000 |^3P_2 0\rangle \\
 & - 0.0020 |^3P_1 0\rangle + 0.0000 |^3P_0 0\rangle - 0.0670 |^1I_6 6\rangle \\
 & - 0.0000 |^1I_6 0\rangle + 0.0670 |^1I_6 -6\rangle + 0.0000 |^1G_4 0\rangle \\
 & - 0.0000 |^1D_2 0\rangle - 0.0000 |^1S_0 0\rangle
 \end{aligned}
 \left. \vphantom{\Phi_6} \right\} W_6^{(0)} = 219 \text{ cm}^{-1}$$

$$\begin{aligned}
 \Phi_7 = & 0.6944 |^3H_6 6\rangle - 0.1632 |^3H_6 0\rangle + 0.6944 |^3H_6 -6\rangle \\
 & + 0.0000 |^3H_5 0\rangle + 0.0028 |^3H_4 0\rangle + 0.0000 |^3F_4 0\rangle \\
 & - 0.0079 |^3F_3 0\rangle + 0.0000 |^3F_2 0\rangle + 0.0000 |^3P_2 0\rangle \\
 & - 0.0020 |^3P_1 0\rangle + 0.0000 |^3P_0 0\rangle - 0.0670 |^1I_6 6\rangle \\
 & - 0.0000 |^1I_6 0\rangle + 0.0670 |^1I_6 -6\rangle + 0.0000 |^1G_4 0\rangle \\
 & - 0.0000 |^1D_2 0\rangle - 0.0000 |^1S_0 0\rangle
 \end{aligned}
 \left. \vphantom{\Phi_7} \right\} W_7^{(0)} = 224 \text{ cm}^{-1}$$

$$\begin{aligned}
 \Phi_8 = & -0.4327 |^3H_6 2\rangle + 0.8961 |^3H_6 -4\rangle - 0.0121 |^3H_5 2\rangle \\
 & + 0.0020 |^3H_5 -4\rangle + 0.0007 |^3H_4 2\rangle + 0.0013 |^3H_4 -4\rangle \\
 & + 0.0070 |^3F_4 2\rangle - 0.0197 |^3F_4 -4\rangle - 0.0040 |^3F_3 2\rangle \\
 & + 0.0026 |^3F_2 2\rangle + 0.0011 |^3P_2 2\rangle - 0.0417 |^1I_6 2\rangle \\
 & + 0.0864 |^1I_6 -4\rangle + 0.0019 |^1G_4 2\rangle - 0.0076 |^1G_4 -4\rangle \\
 & - 0.0007 |^1D_2 2\rangle
 \end{aligned}
 \left. \vphantom{\Phi_8} \right\} W_8^{(0)} = 278 \text{ cm}^{-1}$$

$$\begin{aligned}
 \Phi_{8'} = & -0.4327 |^3H_6 -2\rangle + 0.8961 |^3H_6 4\rangle - 0.0121 |^3H_5 -2\rangle \\
 & + 0.0020 |^3H_5 4\rangle + 0.0007 |^3H_4 -2\rangle + 0.0013 |^3H_4 4\rangle \\
 & + 0.0070 |^3F_4 -2\rangle - 0.0197 |^3F_4 4\rangle - 0.0040 |^3F_3 -2\rangle \\
 & + 0.0026 |^3F_2 -2\rangle + 0.0011 |^3P_2 -2\rangle - 0.0417 |^1I_6 -2\rangle \\
 & + 0.0864 |^1I_6 4\rangle + 0.0019 |^1G_4 -2\rangle - 0.0076 |^1G_4 4\rangle \\
 & - 0.0007 |^1D_2 -2\rangle
 \end{aligned}
 \left. \vphantom{\Phi_{8'}} \right\} W_8^{(0)} = 278 \text{ cm}^{-1}$$

$$\begin{aligned}
 \phi_9 = & -0.7037 |^3H_6 3\rangle + 0.7037 |^3H_6 -3\rangle - 0.0072 |^3H_5 3\rangle \\
 & - 0.0072 |^3H_5 -3\rangle - 0.0015 |^3H_4 3\rangle + 0.0015 |^3H_4 -3\rangle \\
 & + 0.0089 |^3F_4 3\rangle - 0.0089 |^3F_4 -3\rangle - 0.0068 |^3F_3 3\rangle \\
 & - 0.0068 |^3F_3 -3\rangle - 0.0680 |^1I_6 3\rangle + 0.0680 |^1I_6 -3\rangle \\
 & + 0.0040 |^1G_4 3\rangle - 0.0040 |^1G_4 -3\rangle
 \end{aligned}$$

$$W_9^{(0)} = 305 \text{ cm}^{-1}$$

III.3. INTERPRETATION OF THE OPTICAL SPECTRA,  
MAGNETIC SUSCEPTIBILITY AND g-VALUE  
OF PRASEODYMIUM ETHYL SULPHATE

III.3.1. INTRODUCTION

In this section we aim at a consistent interpretation of the magnetic susceptibility, optical absorption spectra and e.p.r data of praseodymium ethyl sulphate (Pr.ES) . Previous workers have reported different values of some parameters to interpret the different experimental results such as optical absorption<sup>117,118</sup>, magnetic susceptibility and anisotropy. We shall investigate to what extent it is possible to interpret the available optical, magnetic susceptibility and e.p.r data simultaneously with a unique set of parameters. The diagonalisation of the complete Hamiltonian consisting of interelectronic repulsion (ES), spin-orbit interaction (SO) and the crystal field interaction (CF) considered together has been carried out. The full J-mixing is thus taken into account. The same type of treatment was done by Gruber to interpret the optical data of Pr.ES. and he deduced the ES parameters ( $F_2$  ,  $F_4$  ,  $F_6$ ) SO coupling constant ( $\zeta$ ) and CF parameters by fitting a large number of optical levels to within 0.1%. But he did not test whether his parameters deduced from optical data were consistent with the magnetic

susceptibility and e.p.r data. It is to be noted that e.p.r, optical absorption and magnetic measurements were not performed with the identical samples of Pr.ES. The e.p.r experiment was performed at low temperature for  $\text{Pr}^{3+}$  in yttrium ethyl sulphate<sup>119</sup>. The optical absorption experiment for concentrated crystal of Pr.ES. was done by Hufner<sup>117</sup>. For diluted crystal of  $\text{Pr}^{3+}$ , the same experiment was done by Hellwege et al<sup>120</sup> and by Gruber<sup>118</sup>. The magnetic susceptibility measurements of concentrated crystal of Pr.ES. were performed earlier by Van den Handel<sup>121</sup> and later by Hellwege et al<sup>122</sup> at different temperatures. But nobody made any attempt to fit theoretically the three experiments: optical absorption, magnetic susceptibility and e.p.r measurements of concentrated Pr.ES. with a single set of parameters. This invokes us to reinvestigate the problem systematically.

### III.3.2. CRYSTAL FIELD ENERGY LEVELS

The  $\text{Pr}^{3+}$  ion in Pr.ES. crystal is considered to be in a  $D_{3h}$  symmetry. So the effective hamiltonian of  $\text{Pr}^{3+}$  ion in  $D_{3h}$  site symmetry and in absence of configuration interaction (C.I.) is given by

$$\mathcal{H}_{\text{eff}} = \sum_{i < j} \frac{e^2}{r_{ij}} + \zeta \sum_i l_i \cdot s_i + A_{20} U_0^{(2)} + A_{40} U_0^{(4)} + A_{60} U_0^{(6)} + A_{66} U_6^{(6)} + U_{-6}^{(6)} \quad (\text{III.3.1})$$

Gruber diagonalised the matrix of (III.3.1) in a basis of all the states belonging to  ${}^3\text{PFH}^1\text{SDGI}$  terms of the  $\text{Pr}^{3+}$  ion. But he did not quote the various CF states in his paper which are required to calculate the magnetic susceptibilities and the g-values. So we repeat the diagonalisation of the complete energy matrix. Equation (III.3.1) does not include the term arising from C.I. which has been discussed earlier in chapter I and which was actually introduced by Rajnak and Wybourne<sup>49</sup>. In course of our investigation we find that unless these C.I. terms are included, a satisfactory agreement of the theory with the experiment is not possible. So by introducing the C.I. term the form of  $\mathcal{H}_{\text{eff}}$  becomes

$$\mathcal{H}_{\text{eff}} = \sum_{i \neq j} \frac{e^2}{r_{ij}} + \sum_i l_i \cdot s_i + A_{20} U_0^{(2)} + A_{40} U_0^{(4)} + A_{60} U_0^{(6)} \\ + A_{66} (U_6^{(6)} + U_{-6}^{(6)}) + \alpha L(L+1) + \beta G(G_2) + \gamma G(R_7) \quad (\text{III.3.2})$$

where  $G(G_2)$  and  $G(R_7)$  are the eigen values of Casimir's operators for the groups  $G_2$  and  $R_7$  used to classify the states of  $f^n$  configuration. These eigenvalues may be calculated in terms of the integers  $(u_1 u_2)$  and  $(w_1 w_2 w_3)$  used to label the irreducible representations of the groups  $G_2$  and  $R_7$  and are tabulated by Wybourne<sup>102</sup>. We use those values.  $\alpha$ ,  $\beta$ ,  $\gamma$  are to be treated as adjustable parameters. In both the above equations  $A_{kq}$ 's are the crystal field parameters in tensor operator form and  $U_q^{(k)}$  is the irreducible tensor operator.

The matrix elements of (III.3.1) or (III.3.2) were obtained by the same procedure as was mentioned in section III.2 .

### III.3.3. COVALENCY REDUCTION OF ORBITAL ANGULAR MOMENTUM

We find that (as in the case of NES) it is impossible to achieve a good fit to the g-values and magnetic susceptibilities unless a reduction of the orbital angular momentum is used in the calculation of these quantities. So a small covalency reduction is introduced here to fit the experimental results. The details of the covalency reduction of the orbital angular momentum has been discussed earlier (chapter II).

### III.3.4. CALCULATION OF THE PARAMAGNETIC SUSCEPTIBILITY

Significant contribution to the magnetic susceptibility of  $\text{Pr}^{3+}$  comes from only the lowest multiplet of  ${}^3\text{H}_4$  .  ${}^3\text{H}_4$  contains 9 crystal field states of which 3 are doublets and 3 are singlets. The paramagnetic ionic susceptibility at different temperatures is obtained from Van Vleck's expression as given in chapter II. The 9CF states are given in Appendix III.3 at the end of this section.

### III.3.5. CALCULATION OF g-VALUES

For the calculation of principal g-values one is interested only in the lowest doublet ( $\phi_1$  ,  $\phi_1'$ ) in the CF level

pattern. With the introduction of the covalency reduction factors ( $k_{\parallel}$  and  $k_{\perp}$ ) for the orbital angular momentum operator, the expressions for the g-values are

$$g_{\parallel} = g_z = \left| \langle \Phi_1 | k_{\parallel} L_z + 2S_z | \Phi_1 \rangle - \langle \Phi_1' | k_{\parallel} L_z + 2S_z | \Phi_1' \rangle \right|,$$

$$g_{\perp} = g_x = g_y = 2 \left| \langle \Phi_1 | k_{\perp} L_x + 2S_x | \Phi_1 \rangle \right| = 2 \left| \langle \Phi_1 | k_{\perp} L_y + 2S_y | \Phi_1 \rangle \right| \\ = 0$$

### III.3.6. RESULTS AND DISCUSSION

Before we start interpreting the experimental data with the present theory it should be noted that the e.p.r, optical absorption and magnetic measurements were not performed with identical samples of Pr.ES. The e.p.r experiment was performed at low temperature for  $\text{Pr}^{3+}$  in Yttrium ethyl sulphate<sup>119</sup>. There are three sets of optical data that are available, one for the concentrated crystal of Pr.ES.<sup>117</sup> and two others for the diluted crystals of  $\text{Pr}^{3+}$  in lanthanum ethyl sulphate<sup>118,120</sup>. Magnetic measurements at different temperatures were however performed for the undiluted crystals of Pr.ES. The levels that could only be observed in the spectrum of concentrated crystals of Pr.ES. are  $^3H_4$ ,  $^3P_1$ ,  $^1I_6$  and  $^3P_2$ . Our aim will be to have a good fit of these levels along with the magnetic susceptibility data, g-value and structural observation.

Earlier Gruber claimed to fit the whole spectrum having a large number of levels by exact diagonalisation of the energy

matrix. He quoted the values of three electrostatic parameters, one spin-orbit coupling parameter and four crystal field parameters. We repeated the calculation as we needed crystal field wave functions. After diagonalising the same matrix with Gruber's set of parameters, we were surprised to observe that not only the centre of gravity of all the levels were shifted but also  $^3P_1$  multiplet goes above the  $^1I_6$  multiplet contrary to Gruber's calculation and experimental findings. Also the position of  $\pm 1$  and 0 components of  $^1I_6$  manifold are reversed. The separation between  $\pm 2$  and 3 components of  $^3H_4$  manifold comes out to be  $17.2 \text{ cm}^{-1}$  against  $12.2 \text{ cm}^{-1}$  as quoted by Gruber. The separation between  $\pm 2$  and 3 components plays an important role in the calculation of the susceptibility. So at this stage we are unable to find any reason for having results different from those of Gruber even though calculation with identical set of parameters was done. When the results obtained from CF calculations by using Gruber's set of parameters are used further for g-value and magnetic susceptibility calculation, it is found that the g-value comes out to be large (2.26 compared to the experimental value 1.525), about 48% larger than the observed value. Experimental data shows that at lower temperature  $K_{\parallel}$  is smaller than  $K_{\perp}$  and around 137K the two curves cross over. But unfortunately we could not reproduce it with Gruber's set of parameters. No reversal of anisotropy ( $K_{\perp} - K_{\parallel}$ ) occurs at any temperature in

the entire range from liquid helium upto room temperature, but  $K_{\parallel}$  is smaller than  $K_{\perp}$  throughout the range. It is also noticed that for  $K_{\parallel}$  the calculated values are higher than the experimental one throughout the whole range of temperature. The difference between the observed and the calculated values varies from 102.8% to 5.9%. It is pronounced at low temperature region and it is largest (102.8%) at the lowest temperature of measurement (6.25K). On the other hand in the case of  $K_{\perp}$  this difference between calculated and observed values is less pronounced (varying from 18.5% to 4.2%) and the calculated values are higher than observed values except at the temperatures 6.25K and 12.5K. Now from the large values of  $g_{\parallel}$  and also  $K_{\parallel}$  and  $K_{\perp}$  one may suggest that a covalency reduction should be introduced in the orbital angular momentum. Next introducing covalency reduction for the orbital moment we made exhaustive trials and found that to have an appropriate reduction in  $g_{\parallel}$  value a covalency reduction factor as high as 0.8 should be introduced in the calculation of the  $K_{\parallel}$  and about 0.95 in the  $K_{\perp}$ . The  $g_{\parallel}$  value comes down to within 1% but the deviation of the susceptibility still remains as high as 41.7% and the reversal point does not occur. Thus we are unable to fit the susceptibility data even within 10% with Gruber's set.

While fitting the observed splitting between the crystal field levels of the concentrated crystals of Pr.ES. using

R-S coupling and without doing J-mixing, Hüfner quoted four crystal field parameters. Although such calculation cannot give electrostatic and SO parameter as it concerns with the splitting of individual free ion levels in a crystal field, it was found that fitting of the crystal field splittings was more or less satisfactory. But there were discrepancies in the assignment of the different crystal field components. The lowest crystal field component of ground term  $^3H_4$  according to their calculation was the doublet ( $\bar{\mu} = \pm 1$ ), whereas from the later experiment of Gruber it is the doublet ( $\bar{\mu} = \pm 2$ ) which is lowest. Also in Hüfner's calculation the components 0 and  $\pm 1$  of  $^1I_6$  multiplet and  $\pm 2$  and  $\pm 1$  components of  $^3P_2$  multiplet interchanged their positions when compared with the observed spectra. We first used these CF parameters of Hüfner along with the spectra  $F_2$ ,  $F_4$ ,  $F_6$  and  $\zeta$  of Gruber to diagonalise exactly the full matrix and obtained the g-value and susceptibility. While carrying out the exact diagonalisation the fitting becomes worse, the optical absorption spectra cannot be explained, the lowest CF components of ground level comes out to be a singlet  $\bar{\mu} = 3$  in complete disagreement with the observed spectra.

So it was clear that both Gruber's and Hüfner's parameters were not satisfactory for a consistent study of all the physical properties mentioned earlier. If the theory is made to agree with results of one type of experiment, it deviates

considerably from the other types of experiment. We made an extensive trial method and the following facts were revealed :

- i) It is only possible to fit the theory with all the experimental data within some optimum limit with a single set of parameters but an exact agreement between the theory and all the experiments is too much to be expected.
- ii) To change the centre of gravity of the multiplets, so that all of them come in right order, introduction of C.I. parameters  $\alpha$ ,  $\beta$ ,  $\sqrt{}$  in our calculation becomes imperative.
- iii) The covalency reduction factors ( $k_{\parallel}$  and  $k_{\perp}$ ) for the orbital angular momentum are to be introduced for having a good fit to (a) the g-values, (b) to reproduce the reversal of the anisotropy ( $K_{\perp} - K_{\parallel}$ ) at about 137K, and (c) the susceptibilities within 10% throughout the entire range of temperature.

We use the following set of parameters which gave a good fit to the optical, e.p.r and magnetic susceptibility data :

$$F_2 = 307.5 \text{ cm}^{-1}, F_4 = 50 \text{ cm}^{-1}, F_6 = 5.0 \text{ cm}^{-1}, \zeta = 727.9 \text{ cm}^{-1},$$

$$\alpha = 11.0, \beta = -450.0, \sqrt{=} = 1000.0, B_2^0 \langle r^2 \rangle = 32.94 \text{ cm}^{-1},$$

$$B_4^0 \langle r^4 \rangle = -77.57 \text{ cm}^{-1}, B_6^0 \langle r^6 \rangle = -53.33 \text{ cm}^{-1}, B_6^6 \langle r^6 \rangle = 985.49$$

$$\text{cm}^{-1}, k_{\parallel} = 0.99, k_{\perp} = 0.98 .$$

The set of parameters which were used by Gruber<sup>118</sup> are as follows :

$$F_2 = 307.4 \text{ cm}^{-1}, F_4 = 49.44 \text{ cm}^{-1}, F_6 = 5.138 \text{ cm}^{-1}, \zeta = 727.9$$

$$\text{cm}^{-1}, B_2^0 \langle r^2 \rangle = 15.31 \text{ cm}^{-1}, B_4^0 \langle r^4 \rangle = -88.32 \text{ cm}^{-1}, B_6^0 \langle r^6 \rangle = -48.76$$

$$\text{cm}^{-1}, B_6^6 \langle r^6 \rangle = 548.48 \text{ cm}^{-1} .$$

The set of parameters due to Hüfner<sup>117</sup> are as follows :

$$B_2^0 \langle r^2 \rangle = 23 \text{ cm}^{-1}, B_4^0 \langle r^4 \rangle = -80 \text{ cm}^{-1}, B_6^0 \langle r^6 \rangle = -44 \text{ cm}^{-1}, \\ B_6^6 \langle r^6 \rangle = 695 \text{ cm}^{-1} .$$

In table III.3.1 we have presented the experimental optical levels and also the theoretical levels with different sets of parameters chosen. In the same table we have also placed the results obtained by Gruber from their own calculation. Fig. III.3.1 shows that the maximum deviation in  $K_{\parallel}$  is about 10% and in  $K_{\perp}$  is about 6% from the experimental curve. Our calculated  $g_{\parallel}$  value deviates from the experimental value by 1.3% (the experimental  $g_{\parallel} = 1.52$  and the theoretical  $g_{\parallel}$  is 1.54). The slight discrepancy in  $g_{\parallel}$  value is quite expected as the theoretical value is referred to the concentrated crystal of Pr.ES. but the experimental result obtained for the diluted crystal of Pr.ES. Table III.3.1 shows that there remains slight discrepancies in  $^1I_6$  multiplets and  $^3P_2$  multiplets when we use our own set of parameters. Two components  $\pm 1$  and 0 of  $^1I_6$  manifold have interchanged their positions and two components  $\pm 2$  and  $\pm 1$  of  $^3P_2$  have interchanged their normal positions. These discrepancies cannot be improved by any adjustment of the 13 parameters which we have mentioned earlier. The possible corrections which may improve the results are the following :

i) Small distortion in the crystals of Pr.ES. may exist even at room temperature. A small departure from reflection symmetry in X-Y plane will change the symmetry of the ion from pure  $C_{3h}$  and introduce terms  $Y_4^{+3}$  and  $Y_6^{+3}$  into the crystal potential, i.e. the new potential will be  $C_{3v}$  in which  $A_{43}$ ,  $A_{63}$  parameters will have very low value. Noting that the new potential does not further lift the degeneracy found with pure  $C_{3h}$ , such distortion was suggested by Elliott and Stevens<sup>110</sup> for Ce-ethyl sulphate to interpret simultaneously the temperature variation of susceptibility and the observed g-values, the latter being much less than the values calculated on the assumption of a pure  $C_{3h}$  symmetry. The second one is that we have assumed in our calculation that all the CF parameters are temperature independent. There may be some temperature dependence of the CF parameters.

Finally we conclude that for future refinement of the theory in the light of the above discussion precise and more experimental data for the concentrated crystal, particularly the optical data of the ground manifold are necessary. This will help to calculate the magnetic susceptibilities and the g-values accurately.

All the calculations which have been presented here were done by computer B6700 using a complete program developed by us.

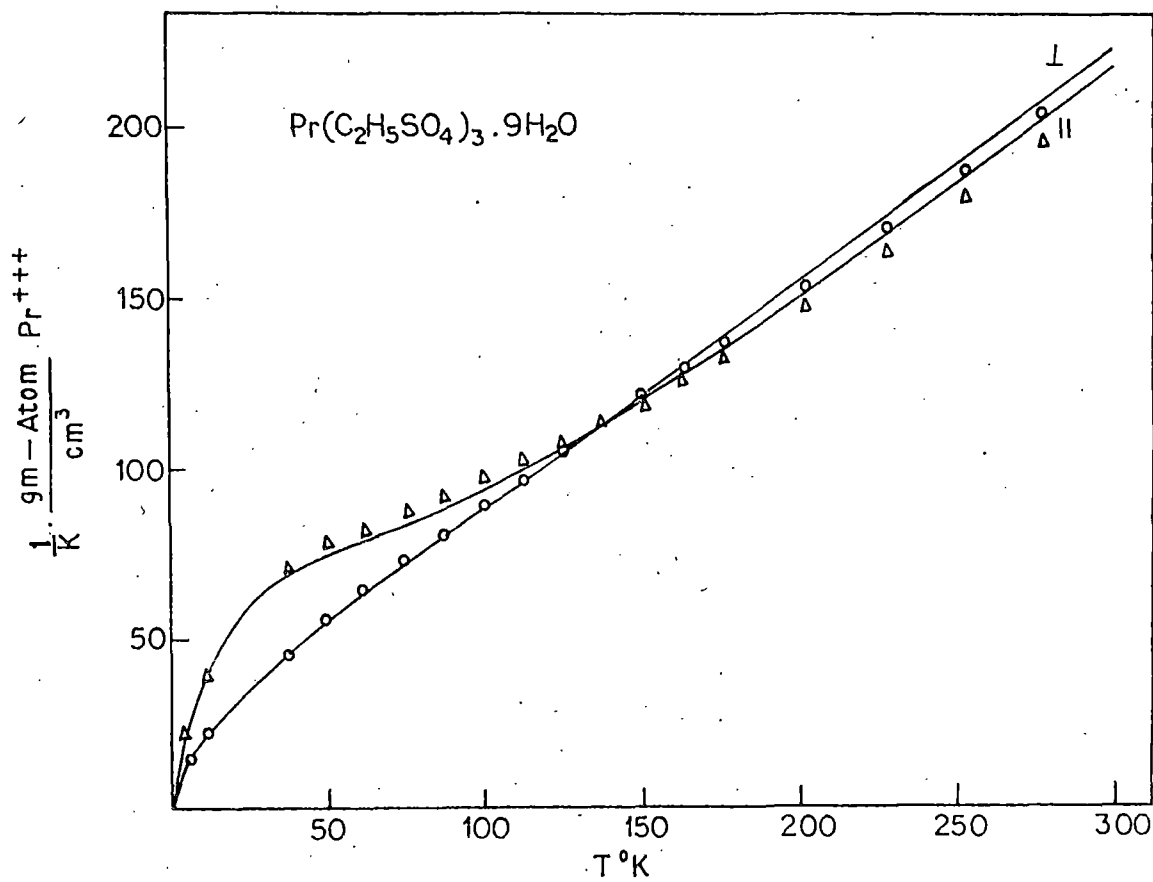


Fig. III.3.1.  $\frac{1}{K_{\parallel}}$  and  $\frac{1}{K_{\perp}}$  of Pr.ES. (gm - atom)  $\text{cm}^{-3}$  at different temperatures (T) in K.

$\Delta, \circ$  Theoretical points.

— Experimental smoothed curve.

Table III.3.1.

Comparison of the experimental and the theoretical crystal field levels

Terms	$\bar{\mu}$	Experimental levels	Theoretical levels obtained from the best fit parameters	Theoretical levels obtained by using Gruber's set of parameters in our calculations	Results obtained from Gruber's <sup>118</sup> original Table II
${}^3H_4$	$\pm 2$	$0^{a,b}$	0	0	0
	3	$11.9^a, 12.2^b$	12	17	15
	$\pm 1$	$(175 \pm 2)^b$	190	172	176
	$\pm 2$	$(188 \pm 28)^a$	303	192	192
	3	$(181 \pm 2)^b$	241	180	181
	0	-	314	288	288
${}^3F_3$	3	-	6345	6266	6330
	0	$6310^b$	6344	6251	6309
	$\pm 2$	$6331^b$	6358	6264	6330
	$\pm 1$	$6383^b$	6417	6317	6383
	3	-	6458	6346	6413
${}^3E_4$	3	-	6917	6763	6767
	3	-	6972	6810	6798
	$\pm 2$	$6831^b$	6990	6841	6825
	$\pm 1$	$6863^b$	7025	6882	6864
	0	$6872^b$	7027	6886	6873
	$\pm 2$	$6896^b$	7060	6916	6895
${}^1G_4$	3	-	9749	9566	9476
	3	-	10091	9804	9736
	0	$9794^b$	10070	9858	9789
	$\pm 2$	$9811^b$	10071	9864	9806
	$\pm 1$	$9863^b$	10162	9930	9867
	$\pm 2$	-	10399	10055	10000
	0	$16709^b$	16994	17051	16724
${}^1D_2$	$\pm 2$	$16858^b$	17144	17184	16857
	$\pm 1$	$16955^b$	17203	17267	16951
	0	$20687^b$	20651	20720	20687
${}^3P_0$	0	$20687^b$	20651	20720	20687
${}^3P_1$	$\pm 1$	$21276^a$	21234	21302	21281
		$21281.1^b$			
	0	$21290^a$	21254	21311	21290
		$21290.6^b$			
${}^1I_6$	0	$21399^a$	21367	20867	21401
	0	$21408^a$	21384	20880	21410
	$\pm 1$	$21447^a$	21426	20909	21443
	0	$21456^a$	21417	20893	21447
	$\pm 2$	-	21515	21009	21540
	$\pm 1$	-	21527	21038	21570
	3	-	21570	21078	21610
	$\pm 2$	-	21639	21138	21672
	3	-	21665	21146	21679
${}^3P_2$	0	$22425^a$	22447	22521	21422
	$\pm 2$	$22441^a$	22473	22524	22443
	$\pm 1$	$22448^a$	22466	22531	22450

<sup>b</sup>Results of diluted crystal of Pr.ES.<sup>117</sup>, <sup>a</sup>Results of concentrated crystal of Pr.ES<sup>118,120</sup>.

APPENDIX III.3.

CF wave functions and the energy values of the ground term ( $^3H_4$ ) of Praseodymium ethyl sulphate obtained from our own set of fitted parameters

$$\begin{aligned} \Phi_1 = & -0.0054 |^3H_6 2\rangle - 0.0188 |^3H_6 -4\rangle - 0.0229 |^3H_5 2\rangle \\ & + 0.0587 |^3H_5 -4\rangle + 0.9066 |^3H_4 2\rangle - 0.3904 |^3H_4 -4\rangle \\ & - 0.0099 |^3F_4 2\rangle - 0.0057 |^3F_4 -4\rangle - 0.0119 |^3F_3 2\rangle \\ & + 0.0314 |^3F_2 -2\rangle + 0.0037 |^3P_2 2\rangle + 0.0008 |^1I_6 2\rangle \\ & + 0.0017 |^1I_6 -4\rangle + 0.1314 |^1G_4 2\rangle - 0.0530 |^1G_4 -4\rangle \\ & + 0.0027 |^1D_2 2\rangle \end{aligned} \left. \vphantom{\Phi_1} \right\} W_1^{(0)} = 0$$

$$\begin{aligned} \Phi_{1'} = & -0.0054 |^3H_6 -2\rangle - 0.0188 |^3H_6 4\rangle - 0.0229 |^3H_5 -2\rangle \\ & + 0.0587 |^3H_5 4\rangle + 0.9066 |^3H_4 -2\rangle - 0.3904 |^3H_4 4\rangle \\ & - 0.0099 |^3F_4 -2\rangle - 0.0057 |^3F_4 4\rangle - 0.0119 |^3F_3 -2\rangle \\ & + 0.0314 |^3F_2 -2\rangle + 0.0037 |^3P_2 -2\rangle + 0.0008 |^1I_6 -2\rangle \\ & + 0.0017 |^1I_6 4\rangle + 0.1314 |^1G_4 -2\rangle - 0.0530 |^1G_4 4\rangle \\ & + 0.0027 |^1D_2 -2\rangle \end{aligned} \left. \vphantom{\Phi_{1'}} \right\} W_1^{(0)} = 0$$

$$\begin{aligned}
 \Phi_2 = & -0.0061 |^3H_6 3\rangle + 0.0061 |^3H_6 -3\rangle + 0.0754 |^3H_5 3\rangle \\
 & + 0.0754 |^3H_5 -3\rangle + 0.6942 |^3H_4 3\rangle - 0.6942 |^3H_4 -3\rangle \\
 & - 0.0198 |^3F_4 3\rangle + 0.0198 |^3F_4 -3\rangle + 0.0308 |^3F_3 3\rangle \\
 & + 0.0308 |^3F_3 -3\rangle + 0.0008 |^1I_6 3\rangle - 0.0008 |^1I_6 -3\rangle \\
 & + 0.1050 |^1G_4 3\rangle - 0.1050 |^1G_4 -3\rangle
 \end{aligned}
 \left. \vphantom{\Phi_2} \right\} W_2^{(0)} = 12 \text{ cm}^{-1}$$

$$\begin{aligned}
 \Phi_3 = & -0.0156 |^3H_6 5\rangle + 0.0079 |^3H_6 -1\rangle - 0.0503 |^3H_5 5\rangle \\
 & + 0.0668 |^3H_5 -1\rangle + 0.9844 |^3H_4 -1\rangle - 0.0267 |^3F_4 -1\rangle \\
 & - 0.0122 |^3F_3 -1\rangle - 0.0113 |^3F_2 -1\rangle - 0.0032 |^3P_2 -1\rangle \\
 & - 0.0034 |^3P_1 -1\rangle + 0.0019 |^1I_6 5\rangle - 0.0012 |^1I_6 -1\rangle \\
 & + 0.1502 |^1G_4 -1\rangle - 0.0003 |^1D_2 -1\rangle
 \end{aligned}
 \left. \vphantom{\Phi_3} \right\} W_3^{(0)} = 190 \text{ cm}^{-1}$$

$$\begin{aligned}
 \Phi_3' = & -0.0156 |^3H_6 -5\rangle + 0.0079 |^3H_6 1\rangle - 0.0503 |^3H_5 -5\rangle \\
 & + 0.0668 |^3H_5 1\rangle + 0.9844 |^3H_4 1\rangle - 0.0267 |^3F_4 1\rangle \\
 & - 0.0122 |^3F_3 1\rangle - 0.0113 |^3F_2 1\rangle - 0.0032 |^3P_2 1\rangle \\
 & - 0.0034 |^3P_1 1\rangle + 0.0019 |^1I_6 -5\rangle - 0.0012 |^1I_6 1\rangle \\
 & + 0.1502 |^1G_4 1\rangle - 0.0003 |^1D_2 1\rangle
 \end{aligned}
 \left. \vphantom{\Phi_3'} \right\} W_3^{(0)} = 190 \text{ cm}^{-1}$$

$$\begin{aligned}
 \Phi_4 = & -0.0071 |^3H_6-2\rangle - 0.0019 |^3H_6-4\rangle - 0.0479 |^3H_5-2\rangle \\
 & + 0.0351 |^3H_5-4\rangle + 0.3854 |^3H_4-2\rangle + 0.9066 |^3H_4-4\rangle \\
 & - 0.1091 |^3F_4-2\rangle - 0.0272 |^3F_4-4\rangle - 0.0370 |^3F_3-2\rangle \\
 & - 0.0071 |^3F_2-2\rangle - 0.0043 |^3P_2-2\rangle + 0.0010 |^1I_6-2\rangle \\
 & + 0.0008 |^1I_6-4\rangle + 0.0626 |^1G_4-2\rangle + 0.1395 |^1G_4-4\rangle \\
 & + 0.0005 |^1D_2-2\rangle
 \end{aligned}
 \left. \vphantom{\Phi_4} \right\} W_4^{(0)} = 203 \text{ cm}^{-1}$$

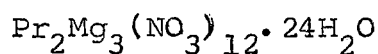
$$\begin{aligned}
 \Phi_{4'} = & -0.0071 |^3H_6-2\rangle - 0.0019 |^3H_6-4\rangle - 0.0479 |^3H_5-2\rangle \\
 & + 0.0351 |^3H_5-4\rangle + 0.3854 |^3H_4-2\rangle + 0.9066 |^3H_4-4\rangle \\
 & - 0.0191 |^3F_4-2\rangle - 0.0272 |^3F_4-4\rangle - 0.0370 |^3F_3-2\rangle \\
 & + 0.0008 |^1I_6-4\rangle + 0.0626 |^1G_4-2\rangle + 0.1395 |^1G_4-4\rangle \\
 & + 0.0005 |^1D_2-2\rangle
 \end{aligned}
 \left. \vphantom{\Phi_{4'}} \right\} W_4^{(0)} = 203 \text{ cm}^{-1}$$

$$\begin{aligned}
 \Phi_5 = & -0.0150 |^3H_6-3\rangle - 0.0150 |^3H_6-3\rangle - 0.0071 |^3H_5-3\rangle \\
 & + 0.0071 |^3H_5-3\rangle + 0.6957 |^3H_4-3\rangle - 0.6957 |^3H_4-3\rangle \\
 & - 0.0424 |^3F_4-3\rangle - 0.0424 |^3F_4-3\rangle - 0.0051 |^3F_3-3\rangle \\
 & + 0.0051 |^3F_3-3\rangle + 0.0025 |^1I_6-3\rangle + 0.0025 |^1I_6-3\rangle \\
 & + 0.1178 |^1G_4-3\rangle + 0.1178 |^1G_4-3\rangle
 \end{aligned}
 \left. \vphantom{\Phi_5} \right\} W_5^{(0)} = 241 \text{ cm}^{-1}$$

$$\begin{aligned}
\Phi_6 = & -0.0121 |^3H_6 6\rangle + 0.0146 |^3H_6 0\rangle - 0.0121 |^3H_6 -6\rangle \\
& -0.0000 |^3H_5 0\rangle + 0.9867 |^3H_4 0\rangle - 0.0373 |^3F_4 0\rangle \\
& + 0.0000 |^3F_3 0\rangle + 0.0027 |^3F_2 0\rangle + 0.0028 |^3P_2 0\rangle \\
& -0.0000 |^3P_1 0\rangle + 0.0049 |^3P_0 0\rangle + 0.0015 |^1I_6 6\rangle \\
& -0.0024 |^1I_6 0\rangle + 0.0015 |^1I_6 -6\rangle + 0.1566 |^1G_4 0\rangle \\
& -0.0006 |^1D_2 0\rangle + 0.0008 |^1S_0 0\rangle
\end{aligned}$$

$$W_6^{(0)} = 314 \text{ cm}^{-1}$$

III.4. STUDY OF THE CRYSTAL FIELD SPECTRA, MAGNETIC  
SUSCEPTIBILITIES AND THE g-VALUES OF



III.4.1. INTRODUCTION

The present section attempts a consistent interpretation of the results of the optical absorption experiment, the magnetic susceptibility measurement and the g-values of  $\text{Pr}_2\text{Mg}_3(\text{NO}_3)_{12} \cdot 24\text{H}_2\text{O}$  (Pr.DN.) with the help of a single set of parameters. Here we have presented a rigorous theoretical approach to the problem. The optical absorption experiment of Pr.DN. was performed by Hellwege and Hellwege<sup>123</sup>. They performed their experiment at about 58K and observed certain crystal field levels. Later Judd<sup>124</sup> tried to explain theoretically the crystal field levels which were obtained by Hellwege and Hellwege<sup>123</sup>. Judd<sup>124</sup> supposed that the rare-earth ion in a double nitrate crystal has a  $C_{3v}$  point group symmetry. He did a first order perturbation calculation for crystal field splitting. Judd was the pioneer worker in the theoretical calculation of crystal field splitting of Pr.DN. He concluded that the Russell-Saunders coupling is totally inadequate to explain the various multiplets. However, he did not carry out the intermediate coupling calculation. The first

order perturbation calculation for the crystal field splitting does not necessarily take into account the J-mixing which has an important role in the crystal field splitting. It is therefore quite natural that such calculation will give only an approximate fit to the crystal field components of the various levels. The first order calculation of the crystal field levels by Judd gave the six crystal field parameters  $A_2^0 \langle r^2 \rangle$ ,  $A_4^0 \langle r^4 \rangle$ ,  $A_6^0 \langle r^6 \rangle$ ,  $A_6^6 \langle r^6 \rangle$ ,  $A_4^3 \langle r^4 \rangle$ ,  $A_6^3 \langle r^6 \rangle$ . The values of the electrostatic parameters  $F_2$ ,  $F_4$ ,  $F_6$  and spin-orbit coupling constant  $\zeta$  cannot be obtained from the first-order calculation.

Cooke and Duffus<sup>90</sup> obtained the  $g_{\parallel}$  value of  $\text{Pr}^{3+}$  diluted in  $\text{La}_2\text{Mg}_3(\text{NO}_3)_{12} \cdot 24\text{H}_2\text{O}$ . The parallel and perpendicular susceptibility measurements of Pr.DN. from 4.4K to 300K were done by Hellwege et al.<sup>125</sup>. But nobody made any attempt to fit the magnetic susceptibility results and the g-value as yet with the values of the parameters that fit the optical absorption results. It was already pointed out by Judd that the parameter deduced by him, using R.S. coupling will not faithfully reproduce the results of optical absorption measurement. Hence, one would therefore cannot expect that simultaneous fitting of the optical, e.p.r and magnetic susceptibility measurements can be made with this set of parameters.

We have presented a rigorous approach which takes into account not only the intermediate coupling but also all possible J-mixing under the crystal field. We have carried out diagonalisation of the matrix of spin-orbit (SO), electrostatic (ES) and crystal field (CF) interaction considered together, the matrix being constructed in a basis of all states of  $\text{Pr}^{3+}$  in  $4f^2$  configuration. This takes into account the full J-mixing. When the parameters given by Judd were used in such calculation it is found that not only the optical levels deviate from the experimental results (see table III.4.1), but also the g-value and susceptibility results deviate considerably from the observed values, the g-value comes out to be  $g_{\parallel} = 1.26$  against the experimental  $g_{\parallel} = 1.55$  and maximum deviations of the parallel and perpendicular susceptibility from the experimental value come out to be about 17% and 51% respectively.

The aim of this chapter is to see whether it is possible to interpret the optical data, the magnetic susceptibility results and the g-value of Pr.DN. with a single set of parameters which gives a good fit to these experiments simultaneously.<sup>126</sup>

### III.4.2. CRYSTALLOGRAPHIC BACKGROUND

The detailed X-ray crystallographic study of  $\text{Ce}_2\text{Mg}_3(\text{NO}_3)_{12} \cdot 24\text{H}_2\text{O}$  has been carried out by Zalkin et al<sup>127</sup>.  $\text{Pr}_2\text{Mg}_3(\text{NO}_3)_{12} \cdot$

$24\text{H}_2\text{O}$  is considered to be isomorphous to the cerium crystal. The crystals are rhombohedral, space group is  $R\bar{3}$ . The lanthanide ion is surrounded by twelve oxygen atoms at an average distance of 0.264 nm. These atoms belonging to six nitrate ions, are at the corners of a somewhat irregular icosahedron. The Mg atoms are of two kinds, each surrounded by six water molecules whose oxygen atoms lie at the corners of an octahedron with Mg-O distance of 0.207 nm (see Fig. III.4.1). The site symmetry at the lanthanide ion found by Zalkin et al<sup>127</sup> (Fig. III.4.2) is  $C_3$ . But the spectroscopic and the resonance data have mostly been interpreted assuming the symmetry to be  $C_{3v}$ . Later Devine<sup>128</sup> suggested that  $T_h$  symmetry is a more realistic approximation to the nearest neighbours of the rare-earth ion than  $C_{3v}$  as there is a complete absence of mirror plane. But  $T_h$  site symmetry disregards the presence of  $A_2^0$  parameter in the crystal field which actually governs the splitting of  $^3P_1$  level. On the other hand the IIa line in the transition  $^3H_4 \rightarrow ^3P_1$  of Pr.DN. is comparatively weak. This led Hellwege and Hellwege<sup>125</sup> to decide on  $C_{3v}$  rather than  $C_3$  for the site symmetry, as an extra selection rule arises owing to the two types of A levels in the irreducible representations of  $C_{3v}$ . Devine also could not fit very well the spectroscopic results of Pr.DN. due to the absence of  $A_2^0$  term in  $T_h$  crystal field.

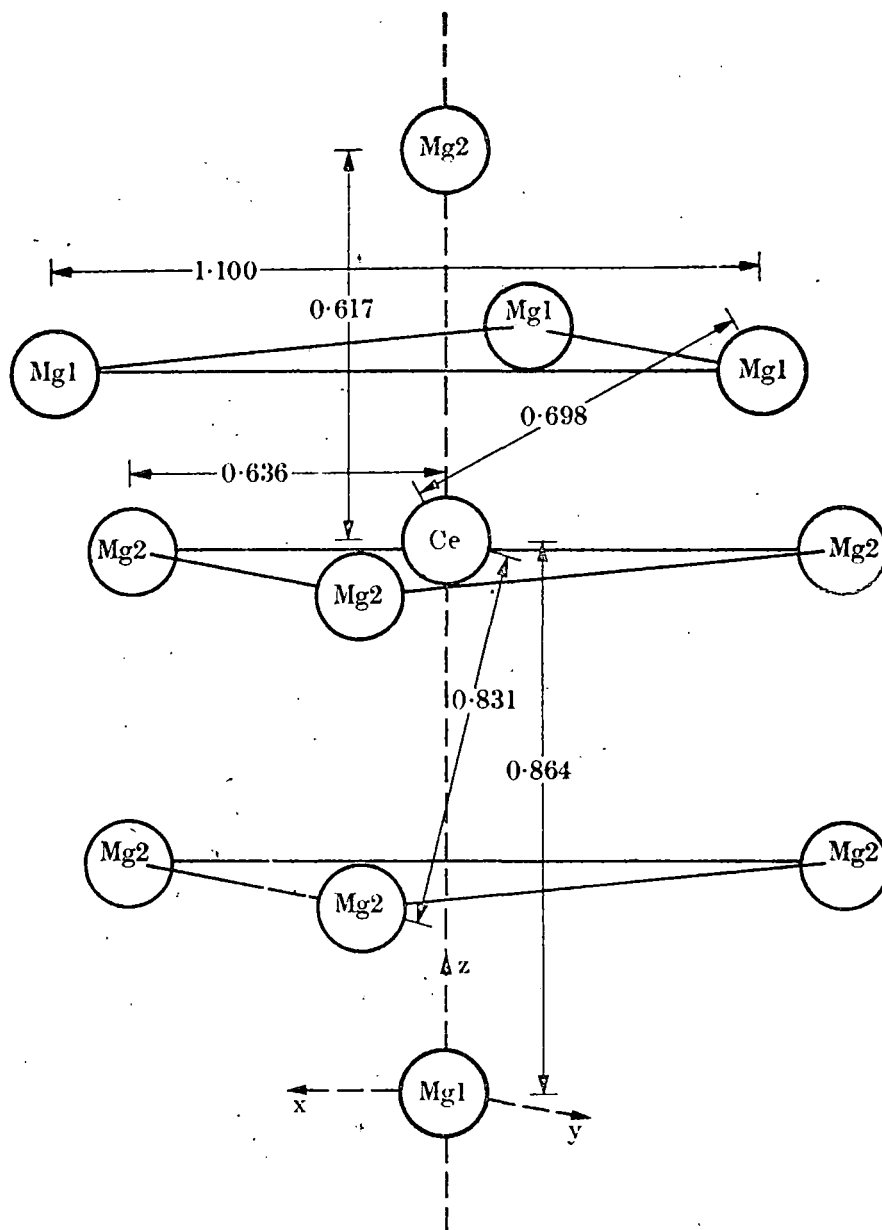


Fig. III.4.1. Positions of the magnesium ions (distances in nanometres) relative to a cerium ion in cerium magnesium nitrate (Zalkin, Forrester and Templeton 1963).

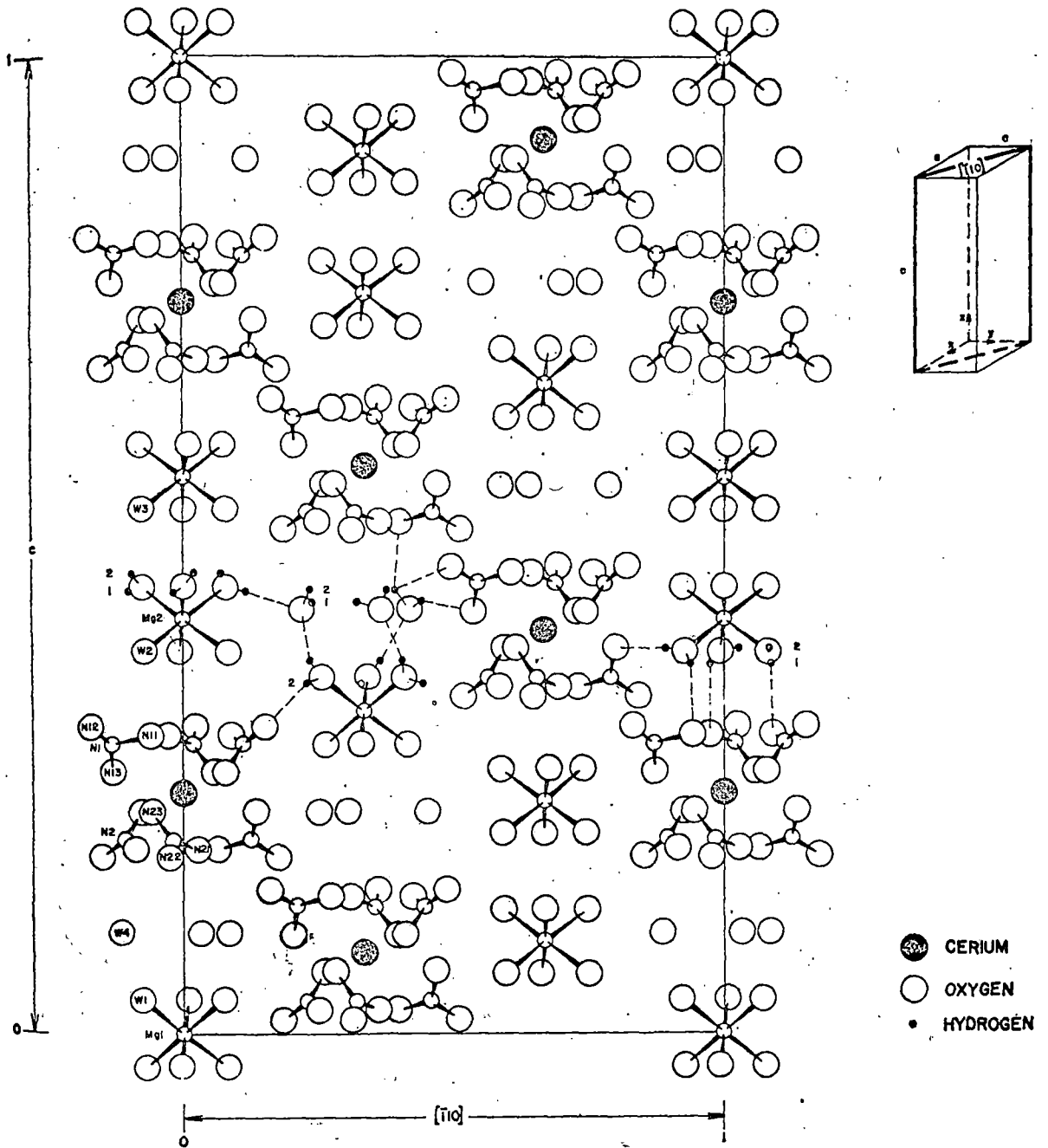
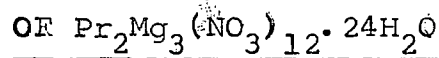


Fig. III.4.2. Crystal structure of  $\text{Ce}_2\text{Mg}_3(\text{NO}_3)_{12} \cdot 24\text{H}_2\text{O}$ . Atoms of Ce and Mg which lie in a section parallel with  $c$  and  $\bar{1}10$  are shown together with nitrate ions and water molecule, near this section. Examples are shown of each kind of hydrogen atom and bond.

So this invokes us to take the site symmetry of Pr.DN. as  $C_{3v}$  where the six order parameters should be of high values in comparison to  $A_{20}$ ,  $A_{40}$ ,  $A_{43}$  parameters. This indicates that the actual symmetry is somewhat a distorted icosahedron having a 3-fold highest symmetry axis.

### III.4.3. INTERPRETATION OF THE SPECTRA



The effective Hamiltonian of  $Pr^{3+}$  in a crystal is given by

$$\mathcal{H}_{\text{eff}} = \sum_{i < j} \frac{e^2}{r_{ij}} + \sum_i b_i \cdot s_i + H_c$$

$H_c$  = crystal field interaction of the 4f electrons with the ligands.

Assuming a  $C_{3v}$  site symmetry  $H_c$  may be written as

$$H_c = A_{20} U_0^{(2)} + A_{40} U_0^{(4)} + A_{60} U_0^{(6)} + A_{66} (U_6^{(6)} + U_{-6}^{(6)}) \\ + A_{43} (U_3^{(4)} - U_{-3}^{(4)}) + A_{63} (U_3^{(6)} - U_{-3}^{(6)})$$

where  $U_q^{(k)} = r^k Y_q^k$  is an irreducible tensor operator.

The crystal field parameter  $A_{kq}$ 's are related with the Stevens parameters  $B_k^q$  by a constant factor. The matrix elements of the effective Hamiltonian  $\mathcal{H}_{\text{eff}}$  is constructed in a basis of states represented by  $|UVSLJM\rangle$ . All states belonging to the different multiplet terms  ${}^3P_{FH}^1SDGI$  have been taken into consideration for the representation of the above matrix

and it turns out to be 91 x 91 matrix. The matrix elements of electrostatic part for  $4f^2$  configuration expressed in terms of Slater-Condon parameters  $F_k$ 's have been tabulated by Nielson and Koster. We use those values. The matrix elements of spin-orbit interaction for  $4f^2$  configuration have also been calculated by Spedding. We use those results of Spedding for  $4f^2$  configuration. The matrix element of  $U_q^k$  was obtained by the same procedure as mentioned in chapter II. Thus the 91x91 matrix is set up. But due to the crystal symmetry the whole matrix splits up into 2 matrices of dimension 30x30 (crystal quantum number  $\bar{\mu} = \pm 1$ ) and one matrix of dimension 31x31 ( $\bar{\mu} = 0$ ).

A computer program was then developed in which the crystal field matrix elements were automatically generated and then added up to SO and ES contribution and after that the three matrices were diagonalised individually giving the crystal field states and corresponding energies. The program was then extended so that the crystal field results can invoke a second portion of the program which automatically calculates the parallel and perpendicular susceptibilities at different temperatures. It also calculates the g-values for the lowest doublet of the ground term  $^3H_4$ .

#### III.4.4. CALCULATION OF g-VALUES

For the calculation of the principal g-values one is interested only in the lowest doublet in the CF level pattern. The two components of the lowest doublet arises from the two 30x30 matrices mentioned above. The components of the lowest doublet are denoted by  $\phi_1$  and  $\phi_1'$ ,

$$g_{\parallel} = g_Z = \left| \langle \phi_1 | L_Z + 2S_Z | \phi_1 \rangle - \langle \phi_1' | L_Z + 2S_Z | \phi_1' \rangle \right|$$

$$g_{\perp} = 2 \left| \langle \phi_1 | L_X + 2S_X | \phi_1' \rangle \right| = 2 \left| \langle \phi_1 | L_Y + 2S_Y | \phi_1' \rangle \right| = 0$$

#### III.4.5. CALCULATION OF PARAMAGNETIC SUSCEPTIBILITY

Significant contribution to the paramagnetic susceptibility of  $\text{Pr}^{3+}$  comes from only the lowest multiplet of  ${}^3\text{H}_4$ .  ${}^3\text{H}_4$  contains 9 crystal field states  $\phi_i$ 's of which 3 are doublets and 3 are singlets. The ionic susceptibility is calculated using the formula (II.11.4) discussed earlier. The 9 CF states are given in Appendix III.4 at the end of this section.

#### III.4.6. RESULTS AND DISCUSSION

We use the following set of parameters which give a good fit to the optical, e.p.r and paramagnetic susceptibility data

$$F_2 = 303 \text{ cm}^{-1}, F_4 = 60.5 \text{ cm}^{-1}, F_6 = 5.65 \text{ cm}^{-1}, \zeta = 730 \text{ cm}^{-1},$$

$$B_2^0 \langle r^2 \rangle = -75.02 \text{ cm}^{-1}, B_4^0 \langle r^4 \rangle = -19.39 \text{ cm}^{-1}, B_6^0 \langle r^6 \rangle = -49.91 \text{ cm}^{-1},$$

$$B_6^6 \langle r^6 \rangle = 702.74 \text{ cm}^{-1}, B_6^3 \langle r^6 \rangle = +2907.92 \text{ cm}^{-1}, B_4^3 \langle r^4 \rangle = \pm 393.3 \text{ cm}^{-1}.$$

The crystal field parameters which were given by Judd as follows

$$B_2^0 \langle r^2 \rangle = -70 \text{ cm}^{-1}, B_4^0 \langle r^4 \rangle = -20 \text{ cm}^{-1}, B_6^0 \langle r^6 \rangle = -50 \text{ cm}^{-1}, \\ B_6^6 \langle r^6 \rangle = 700 \text{ cm}^{-1}, B_6^3 \langle r^6 \rangle = +2300 \text{ cm}^{-1}, B_4^3 \langle r^4 \rangle = +420 \text{ cm}^{-1} .$$

It is found that our values of the three CF parameters  $B_4^0$ ,  $B_6^0$  and  $B_6^6$  differ only very slightly from the corresponding values given by Judd, but the values of the  $B_2^0$  and  $B_4^3$  differ by about 7% from those of Judd, and our value of  $B_6^3$  differs very appreciably from that of Judd by about 26% .

Table III.4.1 shows the calculated and the observed crystal field levels of Pr.DN. The experimental levels which were observed are only  $^3H_4$ ,  $^1D_2$ ,  $^3P_0$ ,  $^3P_1$  and  $^3P_2$  multiplets. Regarding  $^3P_2$  multiplets one should note that Hellwege and Hellwege<sup>123</sup> obtained the two multiplets  $\bar{\mu} = \pm 1$  and  $\bar{\mu} = 0$  within  $3 \text{ cm}^{-1}$ . But it is very much doubtful. Since at that time the optical instrument was not so much sophisticated that this amount of resolution may be reliably done. After an extensive trial with several sets of parameters we also found that it is actually impossible to fit these two levels of  $^3P_2$  as were given by Hellwege and Hellwege. We also found that  $^1D_2$  level could not be fitted very well by any adjustment of the parameters. The discrepancy probably be explained if we consider the effect of configuration interaction on the crystal field

splitting and also the actual site symmetry of  $\text{Pr}^{3+}$  ion in the double nitrate. Other crystal field levels are in close agreement with the experimental levels. The calculated g-values  $g_{\parallel} = 1.58$ ,  $g_{\perp} = 0$  show excellent agreement with the experimental g-values. The calculated  $g_{\parallel}$  value differs from the experimental value only by 0.03. One should also note that the experimental g-value refers to diluted crystal while the theoretical value refers to the concentrated crystal. This may account for the slight discrepancy in the theoretical and experimental g-values. For  $\text{Nd}^{3+}$  in ethyl sulphate<sup>55</sup> crystal, such differences between the diluted and undiluted crystals are already known to exist. Fig. III.4.3 shows the experimental curves for  $\frac{1}{K_{\parallel}}$  and  $\frac{1}{K_{\perp}}$  plotted against temperature along with the theoretical values at intervals of 20K. It clearly shows an overall good agreement between the theoretical and experimental susceptibility values over a wide range of temperatures with a maximum deviations of about 10% for  $K_{\perp}$  and 4% for  $K_{\parallel}$ .

So we find that  $C_{3v}$  symmetry can successfully explain g-values the optical and magnetic data of Pr.DN. On the other hand  $T_h$  site symmetry as assumed by Devine will not be able to account for the splitting of  $^3P_1$ . This splitting entirely depends on the parameter  $B_2^0$  which does not exist in the  $T_h$  symmetry. There may be a slight improvement in the crystal

field levels of Pr.DN. was done by adopting a least square technique. But due to small number in crystal field levels we do not attempt any least square fitting. All calculations presented in this section were done by a complete program developed by us in B6700 computer.

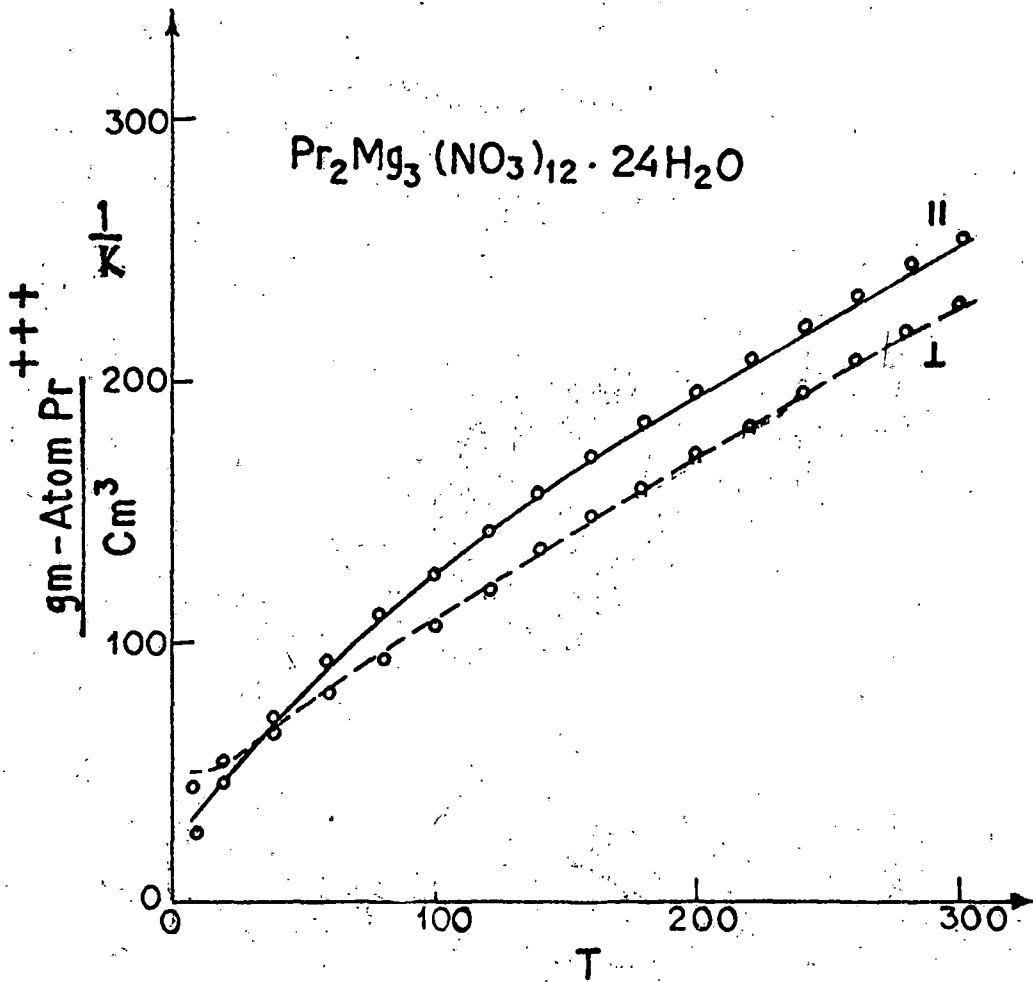


Fig. III.4.3).  $\frac{1}{K_{\parallel}}$  and  $\frac{1}{K_{\perp}}$  of Pr.DN. (gm - atom) $\text{cm}^{-3}$  at different temperatures (T) in  $^{\circ}\text{K}$ .  
 ○ Theoretical points.  
 — and — — Experimental curve.

Table III.4.1.

Comparison between the calculated and experimental values for the crystal field energy levels.

Terms	$\bar{\mu}$	Experimental energy levels in $\text{cm}^{-1}$	Predicted energy levels in $\text{cm}^{-1}$ when our own set of parameters were used	Predicted energy levels when Judd's set of parameters were used
${}^3\text{H}_4$	$\bar{+1}$	0	0	0
	0	38	36.5	31.9
	$\bar{+1}$	96	92.4	56.6
	0	-	419.9	362.4
	0	-	499.5	396.1
	$\bar{+1}$	-	566.5	461.7
${}^1\text{D}_2$	$\bar{+1}$	16872	16888.8	16853.2
	$\bar{+1}$	16920	16965.5	16931.5
	0	16934	17005.5	16930.4
${}^3\text{P}_0$	0	20846	20875.0	20797.1
${}^3\text{P}_1$	0	21422	21409.5	21333.3
	$\bar{+1}$	21461	21453.5	21374.0
${}^3\text{P}_2$	$\bar{+1}$	22630	22650.0	22556.1
	0	22696	22681.9	22598.1
	$\bar{+1}$	22693	22705.1	22605.7

APPENDIX III.4.

CF wave functions and the energy values of the ground term ( $^3H_4$ ) of Praseodymium double nitrate (hydrated) obtained from our own set of fitted parameters

$$\begin{aligned}
 \Phi_1 = & 0.0034 |^3H_6 6\rangle - 0.0365 |^3H_6 3\rangle + 0.0326 |^3H_6 0\rangle \\
 & - 0.0165 |^3H_6 -3\rangle - 0.0787 |^3H_6 -6\rangle - 0.0576 |^3H_5 3\rangle \\
 & + 0.0516 |^3H_5 0\rangle + 0.1013 |^3H_5 -3\rangle + 0.4316 |^3H_4 3\rangle \\
 & + 0.7459 |^3H_4 0\rangle + 0.4659 |^3H_4 -3\rangle + 0.0058 |^3F_4 3\rangle \\
 & + 0.0042 |^3F_4 0\rangle + 0.0076 |^3F_4 -3\rangle + 0.0195 |^3F_3 3\rangle \\
 & + 0.0122 |^3F_3 0\rangle - 0.0200 |^3F_3 -3\rangle - 0.0242 |^3F_2 0\rangle \\
 & - 0.0084 |^3P_2 0\rangle - 0.0070 |^3P_1 0\rangle - 0.0003 |^3P_0 0\rangle \\
 & - 0.0003 |^1I_6 6\rangle + 0.0032 |^1I_6 3\rangle - 0.0030 |^1I_6 0\rangle \\
 & + 0.0017 |^1I_6 -3\rangle + 0.0507 |^1I_6 -6\rangle + 0.0889 |^1G_4 3\rangle \\
 & + 0.0541 |^1G_4 0\rangle - 0.0005 |^1G_4 -3\rangle - 0.0016 |^1D_2 0\rangle
 \end{aligned}
 \left. \vphantom{\Phi_1} \right\} W_1^{(0)} = 0$$

$$\begin{aligned}
 \Phi_1 = & 0.0034 |^3H_6 6\rangle - 0.0365 |^3H_6 3\rangle + 0.0326 |^3H_6 0\rangle \\
 & - 0.0165 |^3H_6 -3\rangle - 0.0787 |^3H_6 -6\rangle - 0.0576 |^3H_5 3\rangle \\
 & + 0.0516 |^3H_5 0\rangle + 0.1013 |^3H_5 -3\rangle + 0.4316 |^3H_4 3\rangle \\
 & + 0.7459 |^3H_4 0\rangle + 0.4659 |^3H_4 -3\rangle + 0.0058 |^3F_4 3\rangle \\
 & + 0.0042 |^3F_4 0\rangle + 0.0076 |^3F_4 -3\rangle + 0.0195 |^3F_3 3\rangle \\
 & + 0.0122 |^3F_3 0\rangle - 0.0200 |^3F_3 -3\rangle - 0.0242 |^3F_2 0\rangle \\
 & - 0.0084 |^3P_2 0\rangle - 0.0070 |^3P_1 0\rangle - 0.0003 |^3P_0 0\rangle \\
 & - 0.0003 |^1I_6 3\rangle + 0.0032 |^1I_6 0\rangle - 0.0030 |^1I_6 -3\rangle \\
 & + 0.0017 |^1I_6 -6\rangle + 0.0507 |^1G_4 3\rangle + 0.0889 |^1G_4 0\rangle \\
 & + 0.0541 |^1G_4 -3\rangle - 0.0005 |^1G_4 -6\rangle - 0.0016 |^1D_2 0\rangle
 \end{aligned}
 \left. \vphantom{\Phi_1} \right\} W_1^{(0)} = 0$$

$$\begin{aligned}
 \Phi_2 = & -0.0278 |^3H_6 6\rangle - 0.0126 |^3H_6 3\rangle - 0.0289 |^3H_6 0\rangle \\
 & + 0.0126 |^3H_6 -3\rangle - 0.0278 |^3H_6 -6\rangle + 0.1070 |^3H_5 3\rangle \\
 & - 0.0000 |^3H_5 0\rangle + 0.1070 |^3H_5 -3\rangle + 0.5252 |^3H_4 3\rangle \\
 & + 0.6387 |^3H_4 0\rangle - 0.5252 |^3H_4 -3\rangle + 0.0067 |^3F_4 3\rangle \\
 & + 0.0026 |^3F_4 0\rangle - 0.0067 |^3F_4 -3\rangle - 0.0197 |^3F_3 3\rangle \\
 & - 0.0000 |^3F_3 0\rangle - 0.0197 |^3F_3 -3\rangle + 0.0155 |^3F_2 0\rangle \\
 & + 0.0114 |^3P_2 0\rangle + 0.0000 |^3P_1 0\rangle - 0.0005 |^3P_0 0\rangle \\
 & + 0.0026 |^1I_6 6\rangle + 0.0012 |^1I_6 3\rangle + 0.0024 |^1I_6 0\rangle \\
 & - 0.0012 |^1I_6 -3\rangle + 0.0026 |^1I_6 -6\rangle + 0.0620 |^1G_4 3\rangle \\
 & + 0.0762 |^1G_4 0\rangle - 0.0620 |^1G_4 -3\rangle - 0.0008 |^1D_2 0\rangle \\
 & - 0.0001 |^1S_0 0\rangle
 \end{aligned}
 \left. \vphantom{\Phi_2} \right\} W_2^{(0)} = 66.5 \text{ cm}^{-1}$$

$$\begin{aligned}
\bar{\phi}_3 = & -0.0313 |^3H_6 5\rangle + 0.0054 |^3H_6 2\rangle + 0.0199 |^3H_6 -1\rangle \\
& + 0.0254 |^3H_6 -4\rangle + 0.0945 |^3H_5 5\rangle - 0.0196 |^3H_5 2\rangle \\
& + 0.1853 |^3H_5 -1\rangle - 0.0213 |^3H_5 -4\rangle - 0.7929 |^3H_4 2\rangle \\
& + 0.1191 |^3H_4 -1\rangle + 0.5429 |^3H_4 -4\rangle + 0.0158 |^3F_4 2\rangle \\
& - 0.0037 |^3F_4 -1\rangle - 0.0064 |^3F_4 -4\rangle + 0.0088 |^3F_3 2\rangle \\
& - 0.0052 |^3F_3 -1\rangle - 0.0037 |^3F_2 2\rangle + 0.0291 |^3F_2 -1\rangle \\
& - 0.0063 |^3P_2 2\rangle + 0.0105 |^3P_2 -1\rangle - 0.0005 |^3P_1 -1\rangle \\
& + 0.0031 |^1I_6 5\rangle - 0.0002 |^1I_6 2\rangle - 0.0020 |^1I_6 -1\rangle \\
& - 0.0019 |^1I_6 -4\rangle - 0.1003 |^1G_4 2\rangle + 0.0158 |^1G_4 -1\rangle \\
& + 0.0668 |^1G_4 -4\rangle + 0.0008 |^1D_2 2\rangle + 0.0008 |^1D_2 -1\rangle
\end{aligned}$$

$$W_3^{(0)} = 92.4 \text{ cm}^{-1}$$

$$\begin{aligned}
\bar{\phi}_3' = & -0.0313 |^3H_6 -5\rangle + 0.0054 |^3H_6 -2\rangle + 0.0199 |^3H_6 1\rangle \\
& + 0.0254 |^3H_6 4\rangle + 0.0945 |^3H_5 -5\rangle - 0.0196 |^3H_5 -2\rangle \\
& + 0.1853 |^3H_5 1\rangle - 0.0213 |^3H_5 4\rangle - 0.7929 |^3H_4 -2\rangle \\
& + 0.1191 |^3H_4 1\rangle + 0.5429 |^3H_4 4\rangle + 0.0158 |^3F_4 2\rangle \\
& - 0.0037 |^3F_4 1\rangle - 0.0064 |^3F_4 4\rangle + 0.0088 |^3F_3 -2\rangle \\
& - 0.0052 |^3F_3 1\rangle - 0.0037 |^3F_2 -2\rangle + 0.0291 |^3F_2 1\rangle \\
& - 0.0063 |^3P_2 -2\rangle + 0.0105 |^3P_2 1\rangle - 0.0005 |^3P_1 1\rangle \\
& + 0.0031 |^1I_6 -5\rangle - 0.0002 |^1I_6 -2\rangle - 0.0020 |^1I_6 1\rangle \\
& - 0.0019 |^1I_6 4\rangle - 0.1003 |^1G_4 -2\rangle + 0.0158 |^1G_4 1\rangle \\
& + 0.0668 |^1G_4 4\rangle + 0.0008 |^1D_2 -2\rangle + 0.0008 |^1D_2 1\rangle
\end{aligned}$$

$$W_3^{(0)} = 92.4 \text{ cm}^{-1}$$

$$\begin{aligned}
 \Phi_4 = & -0.0155 |^3H_6 6\rangle - 0.0016 |^3H_6 3\rangle - 0.0000 |^3H_6 0\rangle \\
 & - 0.0016 |^3H_6 -3\rangle + 0.0155 |^3H_6 -6\rangle + 0.0078 |^3H_5 3\rangle \\
 & + 0.0113 |^3H_5 0\rangle - 0.0078 |^3H_5 -3\rangle + 0.6954 |^3H_4 3\rangle \\
 & - 0.0000 |^3H_4 0\rangle + 0.6954 |^3H_4 -3\rangle - 0.0374 |^3F_4 3\rangle \\
 & + 0.0000 |^3F_4 0\rangle - 0.0374 |^3F_4 -3\rangle - 0.0126 |^3F_3 3\rangle \\
 & - 0.0956 |^3F_3 0\rangle + 0.0126 |^3F_3 -3\rangle + 0.0000 |^3F_2 0\rangle \\
 & + 0.0000 |^3P_2 0\rangle + 0.0014 |^3P_1 0\rangle - 0.0000 |^3P_0 0\rangle \\
 & + 0.0023 |^1I_6 6\rangle + 0.0011 |^1I_6 3\rangle + 0.0000 |^1I_6 0\rangle \\
 & + 0.0011 |^1I_6 -3\rangle - 0.0023 |^1I_6 -6\rangle + 0.0993 |^1G_4 3\rangle \\
 & + 0.0000 |^1G_4 0\rangle + 0.0993 |^1G_4 -3\rangle - 0.0000 |^1D_2 0\rangle \\
 & - 0.0000 |^1S_0 0\rangle
 \end{aligned}
 \left. \vphantom{\Phi_4} \right\} w_4^{(0)} = 419.9 \text{ cm}^{-1}$$

$$\begin{aligned}
 \Phi_5 = & -0.0059 |^3H_6 6\rangle + 0.0083 |^3H_6 3\rangle - 0.0171 |^3H_6 0\rangle \\
 & - 0.0083 |^3H_6 -3\rangle - 0.0059 |^3H_6 -6\rangle - 0.0258 |^3H_5 3\rangle \\
 & - 0.0000 |^3H_5 0\rangle - 0.0258 |^3H_5 -3\rangle + 0.4565 |^3H_4 3\rangle \\
 & - 0.7398 |^3H_4 0\rangle - 0.4565 |^3H_4 -3\rangle - 0.0296 |^3F_4 3\rangle \\
 & + 0.0571 |^3F_4 0\rangle + 0.0297 |^3F_4 -3\rangle + 0.0571 |^3F_3 3\rangle \\
 & - 0.0000 |^3F_3 0\rangle + 0.0571 |^3F_3 -3\rangle + 0.0272 |^3F_2 0\rangle \\
 & + 0.0034 |^3P_2 0\rangle - 0.0000 |^3P_1 0\rangle - 0.0018 |^3P_0 0\rangle \\
 & + 0.0007 |^1I_6 6\rangle - 0.0013 |^1I_6 3\rangle + 0.0037 |^1I_6 0\rangle \\
 & + 0.0013 |^1I_6 -3\rangle + 0.0007 |^1I_6 -6\rangle + 0.0681 |^1G_4 3\rangle \\
 & - 0.1119 |^1G_4 0\rangle - 0.0681 |^1G_4 -3\rangle + 0.0023 |^1D_2 0\rangle \\
 & - 0.0003 |^1S_0 0\rangle
 \end{aligned}
 \left. \vphantom{\Phi_5} \right\} w_5^{(0)} = 499.5 \text{ cm}^{-1}$$

$$\begin{aligned}
 \Phi_6 = & -0.0109 |^3H_6 5\rangle - 0.0049 |^3H_6 2\rangle - 0.0139 |^3H_6 -1\rangle \\
 & - 0.0133 |^3H_6 -4\rangle + 0.0297 |^3H_5 5\rangle - 0.0277 |^3H_5 2\rangle \\
 & - 0.0544 |^3H_5 -1\rangle + 0.0500 |^3H_5 -4\rangle - 0.3673 |^3H_4 2\rangle \\
 & + 0.6220 |^3H_4 -1\rangle - 0.6614 |^3H_4 -4\rangle + 0.0262 |^3F_4 2\rangle \\
 & - 0.0501 |^3F_4 -1\rangle + 0.0449 |^3F_4 -4\rangle + 0.0635 |^3F_3 2\rangle \\
 & - 0.0435 |^3F_3 -1\rangle - 0.0082 |^3F_2 2\rangle + 0.0066 |^3F_2 -1\rangle \\
 & - 0.0016 |^3P_2 2\rangle + 0.0009 |^3P_2 -1\rangle + 0.0002 |^3P_1 -1\rangle \\
 & + 0.0022 |^1I_6 5\rangle + 0.0012 |^1I_6 2\rangle + 0.0025 |^1I_6 -1\rangle \\
 & + 0.0016 |^1I_6 -4\rangle - 0.0560 |^1G_4 2\rangle + 0.0952 |^1G_4 -1\rangle \\
 & - 0.0983 |^1G_4 -4\rangle - 0.0003 |^1D_2 2\rangle + 0.0002 |^1D_2 -1\rangle
 \end{aligned}
 \left. \vphantom{\Phi_6} \right\} W_6^{(0)} = 566.5 \text{ cm}^{-1}$$

$$\begin{aligned}
 \Phi_6' = & -0.0109 |^3H_6 -5\rangle - 0.0049 |^3H_6 -2\rangle - 0.0138 |^3H_6 1\rangle \\
 & - 0.0133 |^3H_6 4\rangle + 0.0297 |^3H_5 -5\rangle - 0.0277 |^3H_5 -2\rangle \\
 & - 0.0544 |^3H_5 1\rangle + 0.0500 |^3H_5 4\rangle - 0.3673 |^3H_4 -2\rangle \\
 & + 0.6220 |^3H_4 1\rangle - 0.6614 |^3H_4 4\rangle + 0.0262 |^3F_4 -2\rangle \\
 & - 0.0501 |^3F_4 1\rangle + 0.0449 |^3F_4 4\rangle + 0.0635 |^3F_3 -2\rangle \\
 & - 0.0435 |^3F_3 1\rangle - 0.0082 |^3F_2 -2\rangle + 0.0066 |^3F_2 1\rangle \\
 & - 0.0016 |^3P_2 -2\rangle + 0.0009 |^3P_2 1\rangle + 0.0002 |^3P_1 1\rangle \\
 & + 0.0022 |^1I_6 -5\rangle + 0.0012 |^1I_6 -2\rangle + 0.0025 |^1I_6 1\rangle \\
 & + 0.0016 |^1I_6 4\rangle - 0.0561 |^1G_4 -2\rangle + 0.0952 |^1G_4 1\rangle - 0.0982 |^1G_4 4\rangle \\
 & - 0.0982 |^1G_4 4\rangle - 0.0003 |^1D_2 -2\rangle + 0.0002 |^1D_2 1\rangle
 \end{aligned}
 \left. \vphantom{\Phi_6'} \right\} W_6^{(0)} = 566.5 \text{ cm}^{-1}$$